ANALYSIS AND OPTIMIZATION OF THE WATER-VAPOR ELECTROLYSIS CELL

by 6908

BHUWAN CHANDRA PANDE
B. Tech., I. I. T., Kanpur, 1968

—

A MASTER'S THESIS

submitted in partial fulfillment of the

requirements for the degree

MASTER OF SCIENCE

Department of Chemical Engineering

KANSAS STATE UNIVERSITY

Manhattan, Kansas

1971

Approved by:

L. T. Fan

Major Professor

THIS BOOK
CONTAINS
NUMEROUS PAGES
WITH THE ORIGINAL
PRINTING BEING
SKEWED
DIFFERENTLY FROM
THE TOP OF THE
PAGE TO THE
BOTTOM.

THIS IS AS RECEIVED
FROM THE
CUSTOMER.

TABLE OF CONTENTS

LIST OF TABLES

LIST OF FIGURES

Chapter 1

INTRODUCTION

In order to minimize the weight of spacecraft for advanced space missions it will be especially important to conserve on the weight of the life support system. One subsystem of the life support system which appears feasible at the present time for recovering breathable oxygen from expired and perspired water vapor is the water-vapor electrolysis cell[1.2]. Water vapor electrolysis has been considered almost exclusively as the physico-chemical, as opposed to biological subsystem technique for recovering oxygen from the vapor of the cabin air. Even in those physicochemical life support systems in which oxygen is to be recovered directly from carbon dioxide (e.g. by electrolysing carbon dioxide) rather than indirectly by (e.g. by carbon dioxide reduction in a Sabatier or Bosch reactor), it will still be necessary to recover some oxygen from water vapor in order to fulfill a man's daily requirement of approximately 2 lb. [1.1].

Studies [1.1, 1.2, 1.3, 1.4, 1.5] concerning the water-vapor electrolysis cell have been carried out and are being carried out in various laboratories. These studies have led to the development of a 1/4 man (1/2 lb O_2/day) prototype unit utilizing a sulfuric acid-silica gel matrix. This technique is an acceptable means of providing breathable oxygen, from either perspired and expired water or water reclaimed from carbon dioxide reduction. A water-vapor electrolysis cell operates by passing a humid air stream continuously through one of the two compartments in the cells. Water vapor in the air stream is then absorbed by the immobilized electrolyte sandwiched between two platinum screen electrodes. The absorbed water is subsequently electrolysed generating oxygen at the anode and hydrogen at the cathode. The polarity is

selected so that the oxygen produced enters the air stream and hydrogen is collected. The hydrogen and oxygen are prevented from mixing by a membrane that separates the two compartments.

As a result of experimental studies at various laboratories the water-vapor electrolysis cell concept has reached a status of acceptance as a new approach worthy of serious consideration for advanced life support systems [1.1]. Most of the work so far has been primarily experimental in nature involving various prototype modules [1.3, 1.5]. It has been more or less a trial and error process and no significant advances have been made towards theoretically analyzing the cell performance and trying to arrive at an optimum design.

The objectives of the present study are to model and simulate the performance of water-vapor electrolysis subsystem and to optimize its design in anticipation of future flight prototype development. In chapter three the operating conditions which minimize the total system weight are presented. This two dimensional weight minimization problem with constraints on the variables is solved by using the sequential unconstrained minimization technique [1.6]. In chapter four the absorption chamber of the water vapor electrolysis cell is modeled by a dispersion model. In this chapter the use of Marquardt's method [1.7] to estimate the parameters of the non-linear model is illustrated. In chapter five a model for ionic transport in solid electrolyte matrices is developed. The application of this model with respect to the water vapor electrolysis cell is discussed. Chapter six presents the recommendations on which future research in this area can be based. It highlights some of the interesting problems which have arisen as a result of the present study.

REFERENCES

1.1 Wydeven, T., and Johnson, R. W., "Water Electrolysis: Prospects for the Future," Transactions of ASME: Journal of Engineering for Industry, 531 (1968).

1.2 Wydeven, T., and Smith, E., "Water Vapor Electrolysis," Aerospace Medicine, 38 (10), 1045 (1967).

1.3 Conner, W. J., Greenough, B. M., and Cook, G. M., "Design and Development of a Water-Vapor Electrolysis Unit," NASA R-607 (1966).

1.4 Clifford, J. E., et al., "A Water-Vapor Electrolysis Cell with Phosphoric Acid Electrolyte," Paper No. 670851 Aeronautic and Space Engineering and Manufacturing Meeting, Los Angeles, October 2-6, 1967.

1.5 Clifford, J. E., et al., "A Water-Vapor Electrolysis Cell with Phosphoric Acid Electrolyte," NASA CR-771 (1967).

1.6 Fiacco, A. V. and G. P. McCormick, "The Sequential Unconstrained Minimization Technique, A Primal-Dual Method," Management Science, 10 (2), 360 (1964).

1.7 Marquardt, D. W., "Least Square Estimation of Non-linear Parameters," A Computer Program in Fortran IV. IBM SHARE Library, Distribution Number SDA 3094.01.

Chapter 2

LITERATURE SURVEY

The initial work on recovering oxygen by the electrolysis of water was made during the NASA-General Dynamics/Convair study which provided for the development, fabrication, and testing of the Langley Integrated Life Support System [2.1]. In this work an ion exchange membrane type of electrolysis unit was used with a 25 percent concentration of sulfuric acid in water as the electrolyte. Unit size was based on supplying oxygen requirements for a 4-man crew, or 8 lb. of oxygen per day. The electrolysis unit weighed 187 lb., had a volume of 7 cu. ft., and was made up of three identical modules each containing 16 cells. Gas and liquid flow was parallel in the modules and within the unit. The 16 cells in each module were electrically in series with each module having a constant current power supply in order to maintain the 10 amp. current flow through the cells at 90oF. Current density was 27 amp/ft^2. The operational reliability of this water electrolysis unit was not very good because of leaks and corrosion problems with the sulfuric acid electrolyte [2.3].

In response to a request for proposal issued by the Langley Research Center of NASA in June 1965, Allis-Chalmers' Advanced Electrochemical Products Division designed and fabricated a water electrolysis unit with an asbestos matrix and potassium hydroxide electrolyte [2.2]. The asbestos matrix provided the zero-G capability for the cell operation. Capillary retention of the liquid at the matrix interfaces prevented mixing of the gases and liquids. The four man electrolysis unit weighed 160 lbs. and had a volume of 4.6 cu. ft. Estimated flight hardware would weigh 104 lb. and occupy 2.8 cu. ft. Average cell requirements were 1.59 v to maintain a current density of 100 amp/ft^2.

THIS BOOK CONTAINS NUMEROUS PAGES WITH DIAGRAMS THAT ARE CROOKED COMPARED TO THE REST OF THE INFORMATION ON THE PAGE.

THIS IS AS RECEIVED FROM CUSTOMER.

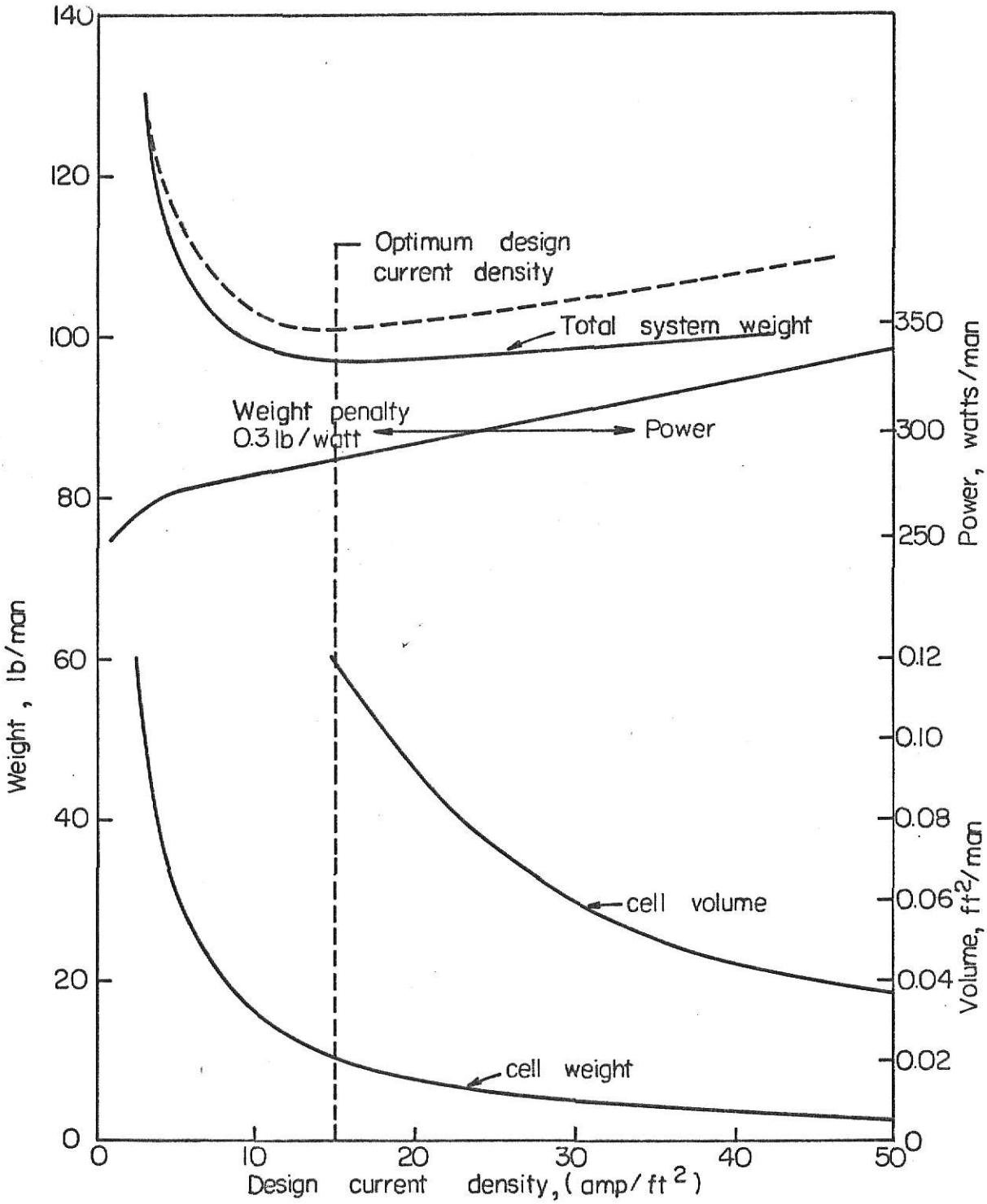

Fig. 2.1. Total system weight for a one man water-vapor electrolysis unit with phosphoric acid electrolyte versus current density.

Water-vapor electrolysis is a new concept in electrolytic oxygen generation in that it operates directly off the humid cabin air [2.8]. The cell can, therefore, assist the cabin air conditioning system in controlling the cabin humidity. Research on the water-vapor electrolysis cell is being conducted at Battelle Memorial Institute and Ames Research Center of NASA. For a concise comparative discussion of the work being done at Battelle and Ames the reader is referred to the paper by Wydeven and Johnson [2.3].

J. E. Clifford et al. [2.4, 2.5] of Battelle Memorial Institute developed a cell which used phosphoric acid as the electrolyte. For zero gravity operation of the cell a matrix of microporous rubber and asbestos impregnated with phosphoric acid was sandwiched between two platinum electrodes. Twelve cells comprised a module which was capable of producing 1/3 of a man's daily requirement of oxygen at the current density of 20 amp/ft^2. The average cell voltage was 2.34 volts and the unit could operate on a 28 v d.c. power supply. For weightless operation the 0.02 in. thick aluminum duct leading to the module contained a 28 v d.c. vane axial blower which directed humid inlet air through the air baffles of the cell. The dimensions of the 12 cell module were approximately 9 x 3.75 x 2.75 in. excluding the air duct and the fan.

One of the most important considerations in designing equipment for spacecraft use is its weight. Every effort should be made during design to minimize the weight requirements. The operating conditions also affect the system and they should be chosen so that the total system weight is minimized. Figure 2.1 shows the relationships between the total system weight and the current density, and also, the weight, volume, and power versus current density relationships for the one man water-vapor electrolysis unit designed

by Battelle [2.5]. The minimum in the total system weight versus current density curve occurs at about 20 amp/sq. ft. which is the optimum design current density for operating the Battelle module.

At the Ames Research Center, W. J. Conner et al. [2.6] developed a water-vapor electrolysis cell which utilized a matrix of sulfuric acid and silica gel. The assembled unit shown in Figure 2.2 included twelve single cells, a cell retainer, an air duct and blower, and a hydrogen header or collector. The dimensions of the unit (excluding the 8-inch long air duct and blower) were 8.0 inches long, 6.5 inches high, and 4 inches deep. The cell retainer, air duct, and blower housing were made of 24 gage light weight aluminum.

Figure 2.3 is an expanded view of the test cell. The gelled electrolyte consisted of a mixture of 8.5 M H_2SO_4 and Cab-O-Sil M-5 (a finely divided form of silica) in a ratio of 10 to 1 by weight. The total volume of the gelled electrolyte in the matrix was 4.5 cm^3. The cathode was an American Cyanamid fuel cell electrode (type AA1). Spot welded to the back (side opposite the gel matrix) of the Cyanamid electrode was a tantalum screen current carrier. The anode was a platinized platinum screen electrode. The active electrode area for the anode and the cathode was 0.0765 ft^2. To prevent the cross leakage of gases within the electrolyte matrix a microporous PVC gas separator was included between the matrix. The membrane was presoaked for several hours in 8.5 M H_2SO_4 before being incorporated into the cell. A compact, variable speed, 28 volt d.c., vane axial blower was used to draw air through the cell.

The curve for the total system weight and weight penalties versus the current density is shown in Figure 2.4 [2.3]. The minimum in the weight for

THIS BOOK CONTAINS SEVERAL DOCUMENTS THAT ARE OF POOR QUALITY DUE TO BEING A PHOTOCOPY OF A PHOTO.

THIS IS AS RECEIVED FROM CUSTOMER.

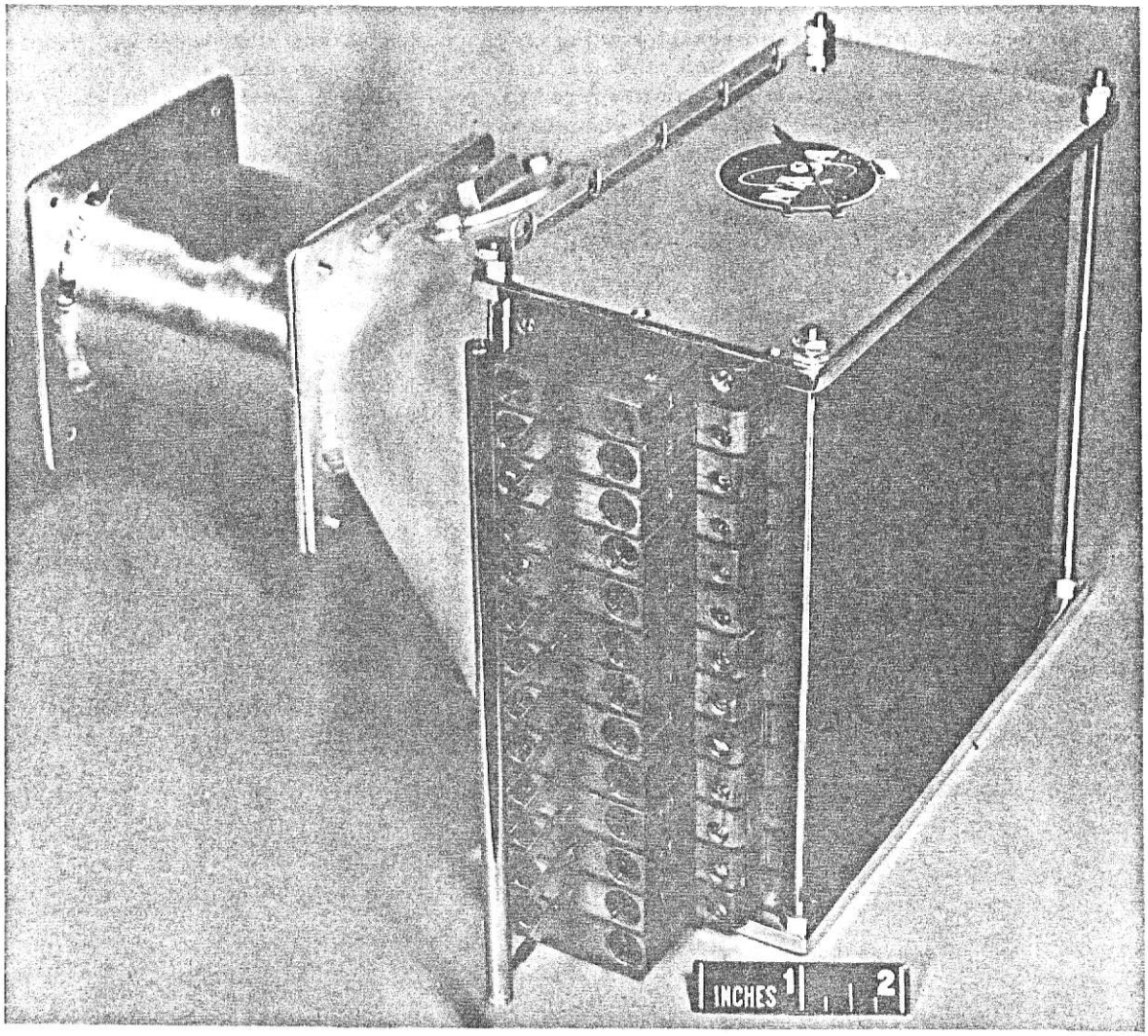

Fig. 2.2 Ames Research Center water-vapor electrolysis cell module of nominal 1/4-man capacity [2,6]

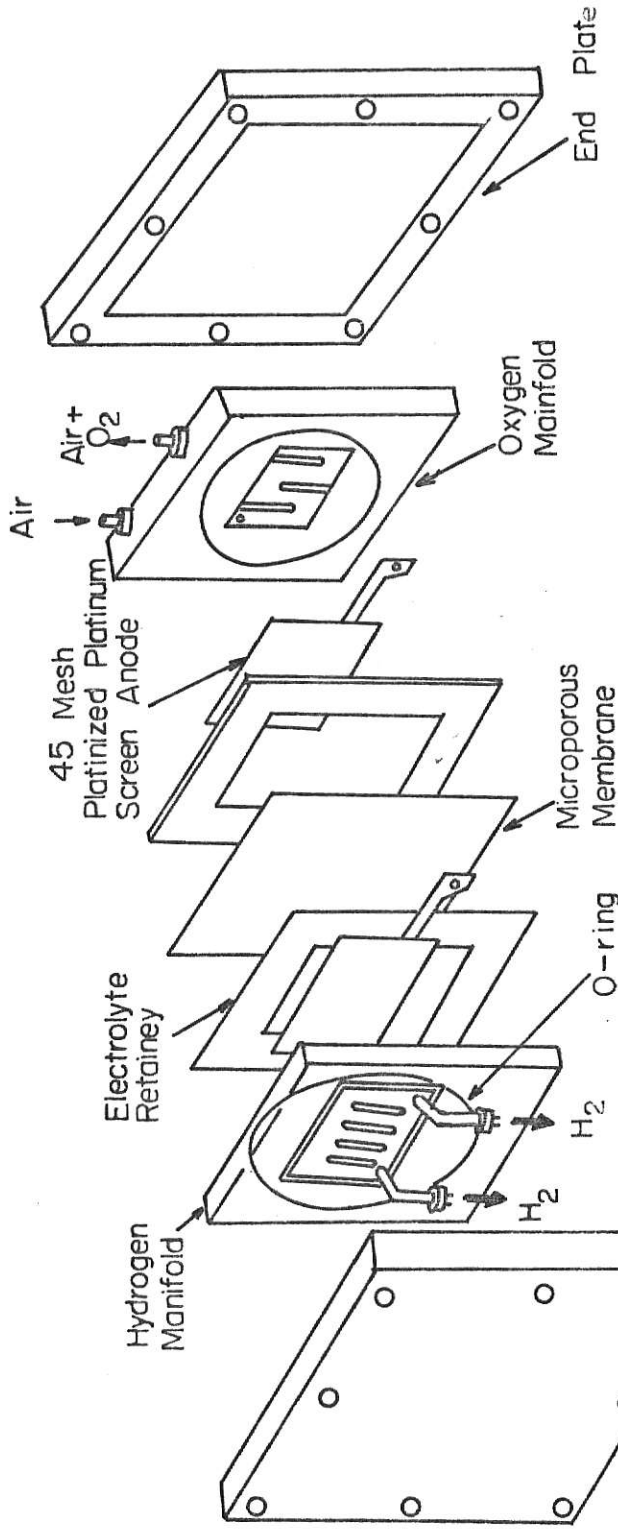

Fig. 2.3. Expanded view of the test cell.

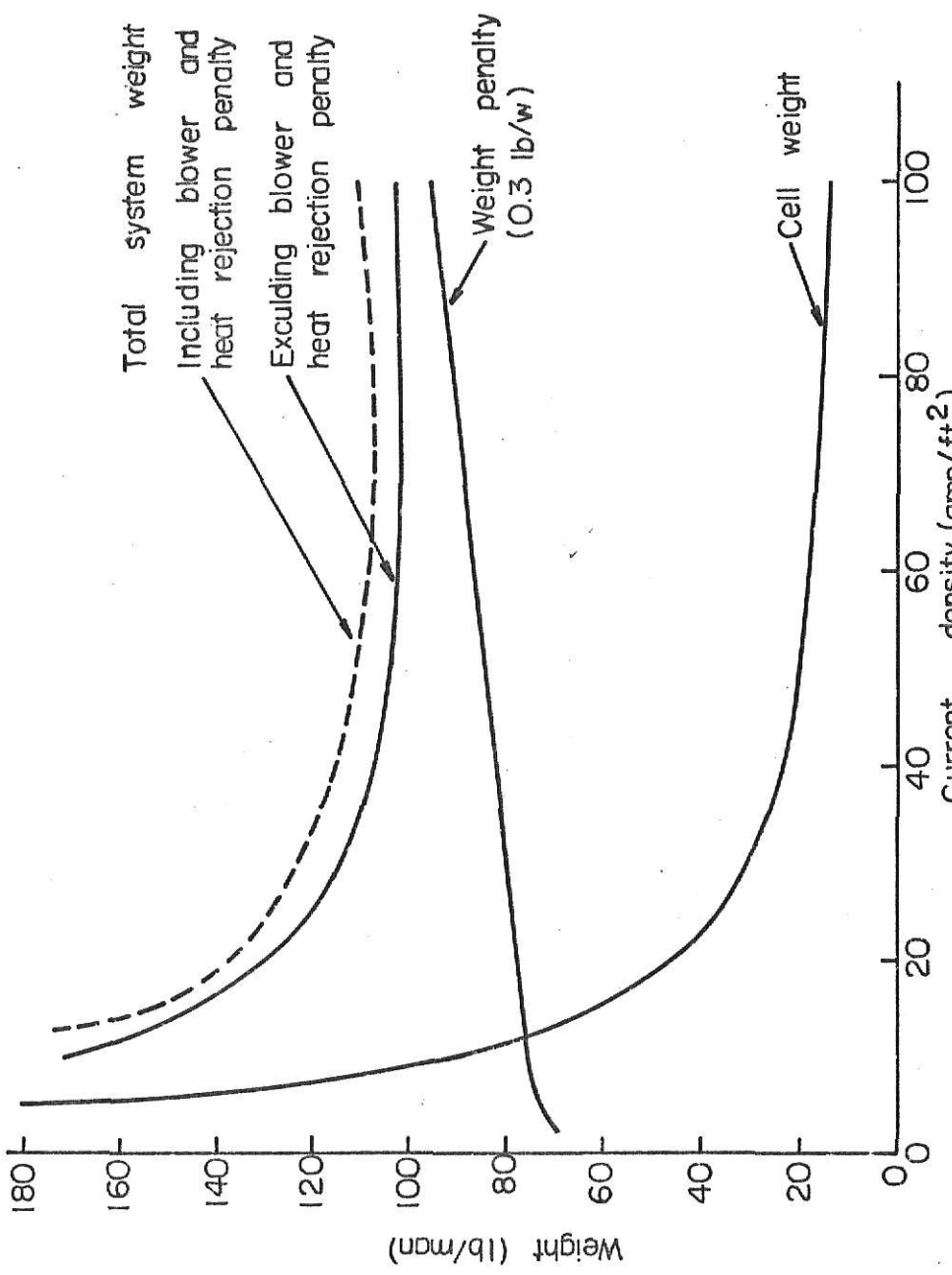

Fig. 24 Total system weight versus current density for the ARC module.

the Ames water-vapor electrolysis cell occurs at about 72 amp./sq. ft. but there is only a small difference in system weight from about 40 to 95 amp./sq. ft. It is unlikely, however, that the sulfuric acid-silica gel system will be run at the optimum current density. The reason is that ozone can be generated at the anode when the anode potential exceeds the reversible potential, E_o, for the half cell reaction [2.3].

$$H_2O + O_2 = 2H^+ + O_3 + 2e, \qquad E_o = +2.07 \text{ v}$$

It is, therefore, necessary to operate the cell at less than the optimum design current density. Another reason is that acid aerosol formation becomes a serious problem at high current densities. For a more detailed discussion of the cell performance and operational difficulties encountered the reader is referred to papers by Wydeven and Johnson [2.3] and Wydeven and Smith [2.8].

The only attempts at modeling and theoretical analysis of the water-vapor electrolysis cell were made by Clifford [2.5] and Engel [2.7]. Both these workers tried to analyze the heat, mass and momentum transfer in the absorption chamber of the electrolyte using theoretical transport equations. The interest is mainly in the temperature and concentration profiles in the air stream under steady state operation. Temperature and concentration gradients in the matrix are represented as variable boundary conditions to the heat and mass transfer equations governing the air stream. The chamber wall opposite the matrix may be regarded as allowing transfer of neither mass nor heat. The chamber has a rectangular cross section, with width much greater than height. Thus, the effects of the side walls may be ignored - reducing the problem to one in two dimensions. Clifford [2.5] obtained the

analytic solutions to the equations of change by assuming a parabolic velocity profile formed by an isothermal, Newtonian fluid infinitely far downstream from the entrance. Engel [2.7] tried to solve the problem by making no assumptions about the velocity profile whatsoever and solving the equations of change numerically.

SUMMARY

A brief survey of the development of water-vapor electrolysis cell has been presented. The good and the bad points of the various electrolysis cell modules have been discussed. Since the cell is still in the developmental stages, most of the work that has been reported is experimental in nature, involving testing of the cell performance under varying conditions and extended periods of time. Some work on the modeling of the cell has been reported.

REFERENCES

2.1 Armstrong, R. C., "Life Support Systems for Space Flights of Extended Time Periods," NASA CR-614 (1966).

2.2 Allis-Chalmers, Advanced Electrochemical Products Division, Milwaukee, Wisconsin, "Design and Development of a Water Electrolysis Unit for an Integrated Life Support System," NASA CR-66654 (1968).

2.3 Wydeven, T. and R. W. Johnson, "Water Electrolysis: Prospect for the Future," Transactions of the ASME: Journal of Engineering for Industry, 531 (1968).

2.4 Clifford, J. E., "Water-Vapor Electrolysis Cell with Phosphoric Acid Electrolyte," Paper No. 670851, Aeronautics and Space Engineering and Manufacturing Meeting, Los Angeles, October 2-6, 1967.

2.5 Clifford, J. E. eta 1., "A Water-Vapor Electrolysis Cell with Phosphoric Acid Electrolyte," NASA CR-771 (1967).

2.6 Conner, W. J., B. M. Greenough and G. M. Cook, "Design and Development of a Water-Vapor Electrolysis Unit," NASA CR-607 (1966).

2.7 Engel, A. J., Private communication.

2.8 Wydeven, T. and E. Smith, "Water Vapor Electrolysis," Aerospace Medicine, 38 (10), 1045 (1967).

Chapter 3

OPTIMIZATION OF SYSTEM WEIGHT

Weight is one of the most important consideration in designing equipment for use in space crafts. A pound of payload requires about a thousand pounds of thrust for lift off and costs about one hundred and fifty thousand dollars in terms of the fuel cost [3.1]. It is imperative, therefore, to achieve as much saving in weight as possible. The saving in weight can be achieved by selecting lightweight cell components and by optimizing operating variables. This includes making use of improved electrode fabrication techniques and using lighter plastic cell parts. Sealing should be emphasized in all designs. For a detailed discussion on this the reader is referred to reports by Conner [3.2] and Clifford [3.5]. Since the system weight depends significantly on the operating variables like temperature and current density, they should be chosen so as to minimize the weight. The minimization of weight with respect to these operating variables will be our main concern in this work.

Some attempts at minimizing the weight were made by W. J. Conner, et al. [3.2] of Lockheed Aircraft Corporation. They considered current density as the only control variable and no constraints were placed in the weight minimization problem. Also they used some of the data obtained for a particular cell and, therefore, their analysis could not be applied to a general case.

In the present work the weight of the cell is minimized by considering the current density and the operating cell temperature as the variables affecting the cell weight. In addition to this, some restrictions are also placed on the system in the form of inequality constraints. These

constraints are placed on the operating variables in order to prevent such phenomena as "flooding", "drying", ozone formation, and excessive overheating. The factors that are considered as contributing to the total system weight are the weight penalty for electrical power consumed, the weight penalty for cooling and the fixed weight of the system. The weight penalties are based on the values supplied by NASA [3.2]. The dimensions of the cell are the same as those of the Ames Research Center module [3.6]. An expression for the weight of the electrolysis cell system is first developed as a function of current density. The temperature dependence is then incorporated using theoretical equations from transport phenomena and electrochemistry. The minimization of this function with inequality constraints is accomplished by using the sequential unconstrained minimization technique (SUMT) [3.7, 3.8, 3.9]. This technique, the algorithm for which was proposed by Fiacco and McCormick [3.8], is based on an idea proposed by C. W. Carrol [3.13] for transforming a minimization problem with constraints into a sequence of unconstrained minimization problems. Calculations have been carried out on the Kansas State University, IBM 360/50 computer using a deck supplied by the Research Analysis Corporation.

DEVELOPMENT OF AN EXPRESSION FOR THE TOTAL SYSTEM WEIGHT AS A FUNCTION OF CURRENT DENSITY

The operating variable that most significantly affects the weight of the electrolysis cell system is the current density. Plots of total system weight versus current density are especially important for electrolysis systems because these plots can be used for determining the optimum current density at which a given electrolysis cell system should be operated. The optimum current density is normally that for which the

total system weight is minimum. In this section we shall derive an expression for the total weight for the water-vapor electrolysis cell system as a function of current density.

The total number of cells required for a one man unit can be calculated from the following equation,

$$N = \frac{I}{A_e i} \tag{3.1}$$

where

N = total number of cells required for a one man unit

I = total current required for a one man unit, amp

A_e = area of each electrode, ft^2

i = current density, amp/ft^2

The expression for the total system weight can be written as

$$W = W_E + W_b + W_c \tag{3.2}$$

where

W = total system weight, lbs

W_E = weight penalty due to electrical power consumed, lbs

W_b = fixed weight of the one man electrolysis unit, lbs

W_c = weight penalty for heat rejection, lbs.

Weight Penality for Electrical Power Consumed.

Electrical power is consumed in providing energy for electrolysis and driving the blower. Let the bank power for electrolysis be denoted

by P_b and the power for driving the blower by P_f. Assuming a power penalty of 0.3 lb/watt [3.2], the weight due to electrical power consumed can be written as

$$W_E = 0.3\ (P_b + P_f N) \tag{3.3}$$

The bank power for electrolysis, P_b, is given by

$$P_b = I \times E \tag{3.4}$$

where E is the cell voltage.

For finding an expression for the blower power, P_f, the flow through the cell can be visualized as a laminar flow between the equivalent broad parallel plates of small spacing (b'). Since the Reynolds number is low (see Appendix IV), the theoretical laminar fluid-flow equations can be used to derive an expression for the pressure drop, ΔP [3.10].

$$\Delta P = \frac{0.35\ q\mu' L}{A_c\ (b')^2} \tag{3.5}$$

where

ΔP = pressure drop in the absorption chamber, p

b' = channel height of absorption chamber, mils

μ' = viscosity of the humid air at $75^{o}F$, centipoise

q_1 = air flow rate, ft^3/sec

L = length of the flow path, in.

A_c = area of cross section for flow of air, ft^2

The flow rate, q, in the above expression is not an independent variable but is determined by the requirements of producing one man's

daily requirement of oxygen and the actual absorption rate over the electrolyte matrix. There is thus a definite relation between the flow rate and the current density for a particular cell geometry. This relation can be obtained as follows:

Since, according to Faraday's law one gram equivalent of an electrolyte must be decomposed for every Faraday of electricity passed, the water electrolysis rate per ampere of the current passing through the cell is

$$\frac{m}{nF} \frac{\text{lb. } H_2O/\text{sec}}{\text{ampere}}$$

where

m = pounds of water decomposed

n = number of equivalents per mole of water

F = Faraday's number, coul./equivalent

The theoretical rate of water electrolysis for any current density i, amp./ft^2, therefore, is

$$r_{we} = \frac{m}{nF} \times A_e i \tag{3.6}$$

r_{we} is the rate of electrolysis of water in lb/sec.

The rate of electrolysis must be equal to the rate of water absorption over the anode by the requirements of continuity. The water absorption process in the chamber is difficult to describe theoretically because there are several factors as the flow rate, concentration of the acid, humidity of the inlet air, geometry of the chamber etc. that influence

it. The difference between the humidity of the inlet air and the water vapor pressure over the acid is the actual driving force for the mass transfer. The driving force for the absorption process is the difference in humidities of the bulk air and that at the air matrix interface. An expression for the rate of absorption as a function of the humidity driving force has been derived in Appendix II, which is based on the data of Figure 3.1. The mass transfer coefficient that has been calculated therein is however a function of the geometry of the cell and the flow characteristics of air and cannot be applied to all cases. The data of Figure 3.1 is for a cell with 8.0M acid electrolyte and an active electrode area of 18 Cm^2. In the ARC module the concentration of the electrolyte is 8.5M and the active electrode area is 70 Cm^2. In order to have an expression which is more general in its applicability, experiments should be done to determine the variation of the mass transfer coefficient with the geometry of the cell and the flow characteristics of air. But in the present work the absorption rate has only been considered as a function of air flow rate and the inlet water humidity has been taken to be constant. This is a much better method than to express the absorption rate as a function of humidity difference driving force and then expressing the mass transfer coefficient as a function of the air flow rate, because this will render the problem unsuitable for optimization. For the purpose of optimizing the weight an empirical expression for the absorption rate based on the experimental studies of Conner et al. [3.2], has been used. This expression was derived for a cell which had an active electrode area of 0.097 ft^2 and is operating at an inlet humidity of 48%. The expression is

$$r_{wa} = 2.06 \times 10 A_e^{5} (q)^{0.644} \qquad (3.7)$$

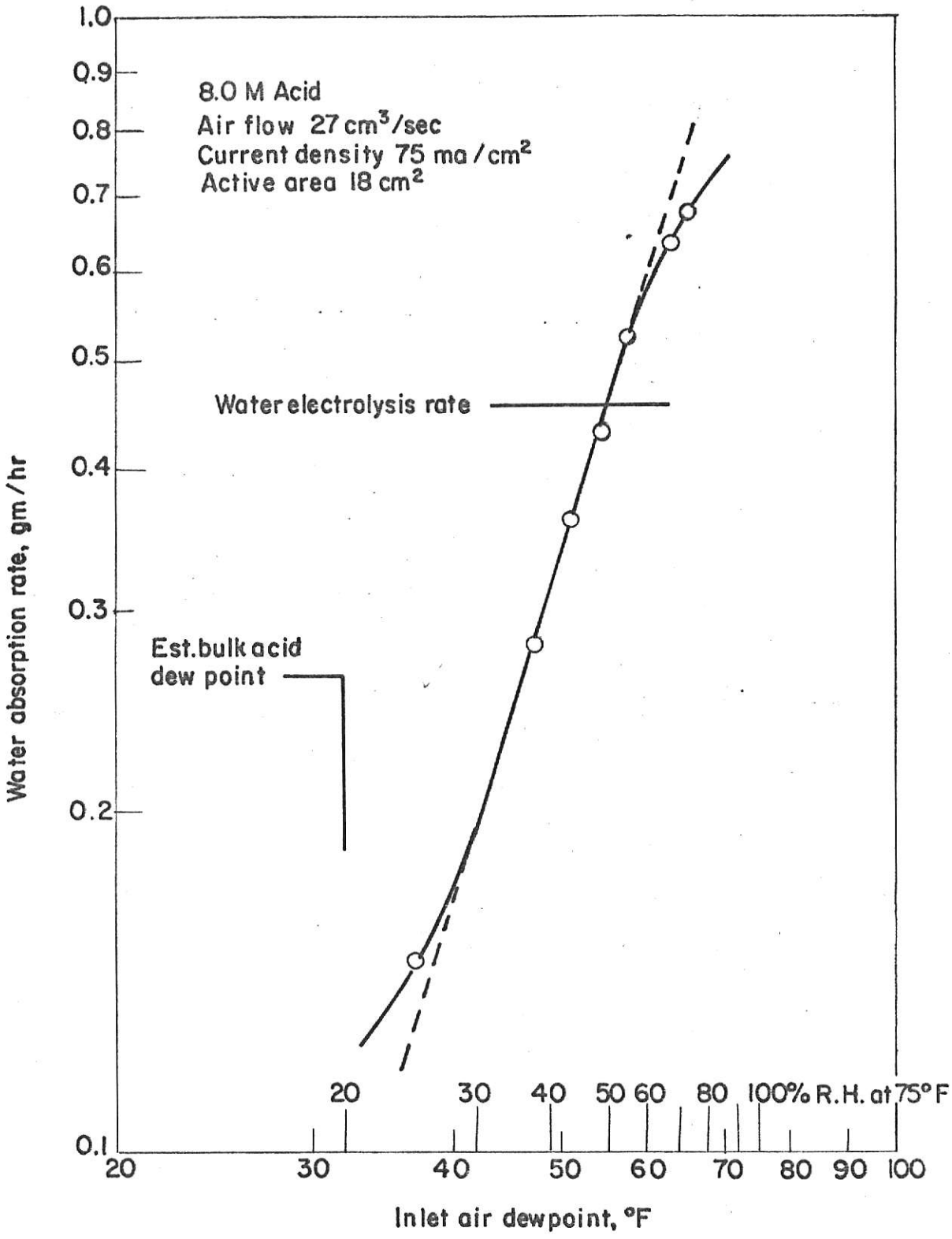

Fig. 3.1. Water absorption with inlet air dewpoint [3.2].

where

r_{wa} = water absorption rate for the cell, lb/sec.

Equating the electrolysis rate, equation (3.6), to the absorption rate, equation (3.7), we have

$$2.06 \times 10^{-5} A_e (q)^{0.644} = \frac{m}{nF} A_e i$$

therefore,

$$q = 1.83 \times 10^{7} \times \left(\frac{m}{nF}\right)^{1.55} i^{1.55} \qquad (3.8)$$

Making use of equation (3.5) and (3.8) and assuming an overall blower efficiency of 50%, the expression for blower power can be written as

$$P_f = \frac{\Delta P x q}{0.5} = \frac{0.35\ q\mu' L}{0.5\ A_c\ (b')^2} \times 144 \times q\ \frac{\text{ft-lb}}{\text{min}}$$

Converting the units to watts and using the expression for q from equation (3.8), the blower power, P_f, may be written as

$$P_f = \frac{0.35 \times 144 \times \mu' L}{0.5 \times A_c\ (b')^2} \times q^2 \times \frac{746}{33{,}000} \text{ watts}$$

$$= \frac{0.35 \times 144 \times \mu' L}{0.5 \times A_c\ (b')^2} \times (1.83)^2 \times 10^{14} \times \left(\frac{m}{nF}\right)^{3.10} i^{3.10} \times \frac{746}{33{,}000}$$

$$= 3.68 \times 10^{14} \frac{\mu' L}{A_c\ (b')^2} \left(\frac{m}{nF}\right)^{3.10} i^{3.10} \qquad (3.9)$$

Substituting the expressions for P_b and P_f from equations (3.4) and (3.9) into equation (3.3), the expression for W_E may be written as

$$W_E = 0.3 \left[I \times E + 3.68 \times 10^{14} \frac{\mu' L}{A_c (b')^2} \left(\frac{m}{nF}\right)^{3.10} i^{3.10} \right] \qquad (3.10)$$

Fixed Weight of the Water Vapor Electrolysis Unit

For a 1/4-man ARC module the cell component weights are given in Table 3.1 [3.11]. From the table it can be seen that the weight of the twelve assembled cells is 3495.5 gms. Therefore, the weight of N assembled cells $= \frac{3495.9}{12} (N)$

$$= 291.3 (N)$$

The fixed weight associated with the twelve cell unit is 1369.9 gm. Assuming that this remains unchanged for a one man unit, the expression for the fixed weight of the one man unit may be written as

$$W_b = 291.3 (N) + 1369.9$$

or in lbs.

$$W_b = 0.62 (N) + 3.02 \qquad (3.11)$$

Weight Penalty for Heat Rejection

It was shown by Conner et al. [3.2] that any cell voltage above 1.48 volts results in the production of heat which must be removed.

The total heat which must be removed from a one man unit, in watts, is

$$P_h = I \times (E - 1.48)$$

Table 3.1. WEIGHTS OF THE CELL COMPONENTS OF 1/4-MAN UNIT [3.11]

Component	Single Cell (gms)	Unit Weight (gms)
Electrodes		
Anode	18.2	
Cathode	18.2	
Matrix		
Gel retainer	13.5	
Silica gel + H_2SO_4	23.0	
Manifolds		
Oxygen (end plate)	226.4	
Hydrogen (end plate)	234.3	
Oxygen-Hydrogen	150.5	
Current distributer (pt. ribbon)	18.1	
Twelve assembled cells		3495.9
Cell retainer + thru bolts		349.9
Fan housing + duct		566.0
Fan		454.0
Total unit weight (12 cells)		4865.8 (10.7#)

Assuming a heat rejection penalty of 0.03 lb/watt, the weight penalty for cooling is

$$W_c = 0.03\ I \times (E - 1.48) \tag{3.12}$$

Total System Weight as a Function of Current Density

The total system weight for the one man unit is the sum of equations (3.10), (3.11) and (3.12), i.e.

$$W = W_E + W_b + W_c$$

or

$$W = 0.3 \left[I \times E + 3.68 \times 10^{14} \times N \frac{\mu' L}{A_c (b')^2} \left(\frac{m}{nF}\right)^{3.10} i^{3.10} \right]$$

$$+ 0.62\ (N) + 3.02 + 0.03\ I \times (E - 1.48) \tag{3.13}$$

An expression for the cell voltage, E, of the ARC module was reported by Clifford, Kim and Kolic [3.6]. The expression is

$$E = 1.822 + 0.171 \log i + 0.002\ i \tag{3.14}$$

Substituting the expressions for E and N from equations (3.14) and (3.1) respectively into equation (3.13) we can express the total system weight, W, only as a function of the current density, i. It should be noted, however, that this expression will be valid only at 75 since equation (3.14) is was arrived at by conducting experiments at $75^{o}F$. The effect of temperature on the total system weight will now be incorporated by studying the effects of temperature on equation (3.14) and other physical properties which are influence by temperature.

EFFECT OF TEMPERATURE

The temperature can effect the total system weight by changing the voltage characteristics of the cell and the blower power. The details of this temperature dependence have been presented below.

Effect on Voltage Characteristics

For the ARC module the average of the voltage characteristics of the twelve cells at $75^{o}F$ may be written as [3.6]

$$E = 1.822 + 0.171 \log i + 0.002 i$$

For analyzing the effect of temperature on the voltage characteristics, the voltage can be broken up into three parts [3.5]:

(a) Open circuit voltage = 1.23 volts

(b) Chemical polarization = $0.59 + 0.171 \log i$

(c) Ohmic polarization = $0.002 i$

The expression for the chemical polarization is given by [3.14]

$$\Delta E_{chem} = a + b \log i \qquad (3.15)$$

The constants a and b are defined by

$$a = - (RT/\alpha nF) \ln i_o \qquad (3.16)$$

$$b = 2.303 (RT/\alpha nF) \qquad (3.17)$$

where

R = gas law constant, cal./(mole)(^{o}K)

T = the absolute temperature, ^{o}K

α = constant referred to as the transfer coefficient, dimensionless

n = number of equivalents per mole, eq./mole

F = Faraday's constant, coul/eq.

i_o = exchange current density, amp/ft^2

Equations (3.16) and (3.17) show that the constants a and b vary linearly with temperature. Therefore,

$$a = a_o T \qquad b = b_o T \tag{3.18}$$

At 75°F, $a = 0.59$ and $b = 0.171$; therefore,

$$a_o = \frac{0.59}{298} = 1.98 \times 10^{-3}$$

$$b_o = \frac{0.171}{298} = 5.74 \times 10^{-4}$$

The open circuit voltage E_o is given by [3.14],

$$E_o = E_t + \frac{RT}{nF} \ln \frac{(P_{H_2})(P_{O_2})^{1/2}}{(P_{H_2O}} \tag{3.19}$$

where

$$E_t = \frac{\Delta F^o}{nf} = \frac{RT}{nF} \ln K_p \tag{3.20}$$

where ΔF^o is the standard free energy of formation and K_p is the equilibrium constant for the reaction

$$H_2O(g) = H_2(g) + \frac{1}{2} O_2(g) \tag{3.21}$$

For the above reaction $\Delta F^o = 54{,}650$ Cal/mole and $K_p = 7.37 \times 10^{39}$ at 25°C. The variation of K_p with temperature is governed by the van't Hoff equation, viz. [3.14]

$$\frac{d}{dT} (\ln K_p) = \frac{\Delta H^o}{RT^2}$$

Integrating this gives

$$\ln K_p = - \frac{\Delta H^o}{RT} + \ln K_{p_o} \tag{3.22}$$

In the above integration ΔH^o has been assumed to be independent of temperature. The value of ΔH^o for the reaction (3.21) is -57.7979 Kcal/mole. Equation (3.22) can, therefore, be written as

$$\ln K_p = \frac{29,060}{T} - 5.71 \tag{3.23}$$

Equation (3.20) cna therefore be written as

$$E_t = 1.25 - 2.46 \times 10^{-4} T \tag{3.24}$$

The changes in gas pressure will have only minor effects on cell voltages. This follows because a tenfold change in P_{H_2}, P_{H_2O} or P_{O_2} will change E_o by less than 0.03 volts, or less than 3 percent [3.5]. The second term in equation (3.19) can therefore be assumed to vary linearly with temperature with a slope of $\frac{R}{nF} \ln \frac{(P_{H_2})(P_{O_2})^{1/2}}{(P_{H_2O}}$. The value of this slope at normal operating conditions is 1.82×10^{-4}. Equation (3.19) can therefore be written as

$$E_o = 1.25 - 0.64 \times 10^{-4} T \tag{3.25}$$

In the absence of experimental data, the variation of resistivity with temperature has been assumed to be negligible. The voltage, characteristics can, therefore, be represented by

$$E = 1.25 + 1.92 \times 10^{-3} T + 5.74 \times 10^{-4} T \log i + 0.002 i \quad (3.26)$$

The variation of voltage characteristic as depicted by this equation is plotted in Figure 3.2.

Effect On Blower Power

Temperature can affect the blower power by making changes in

(a) absorption rate

(b) pressure drop due to change in viscosity of air

The absorption rate is given by equation (3.7). Some experimental studies by Greenough et al. [3.2] show that the temperature has almost negligible effect on the absorption characteristics (see Figure 3.3). The viscosity of air varies as 0.75 power of temperature [3.12], that is,

$$\mu = \frac{\mu'}{(298)^{0.75}} T^{0.75} \quad (3.27)$$

Substituting for μ in equation (3.9)

$$P_f = 3.68 \times 10^{14} \times \frac{\mu' \times T^{0.75}}{(298)^{0.75}} \times \frac{L}{A_c (b')^2} \left(\frac{m}{nF}\right)^{3.10} i^{3.10}$$

$$= 5.1 \times 10^{12} \frac{\mu' L}{A_c (b')^2} \left(\frac{m}{nF}\right)^{3.10} T^{0.75} i^{3.10} \quad (3.28)$$

Total System Weight as a Function of Temperature and Current Density.

Making use of equation (3.28), the total system weight, as a function

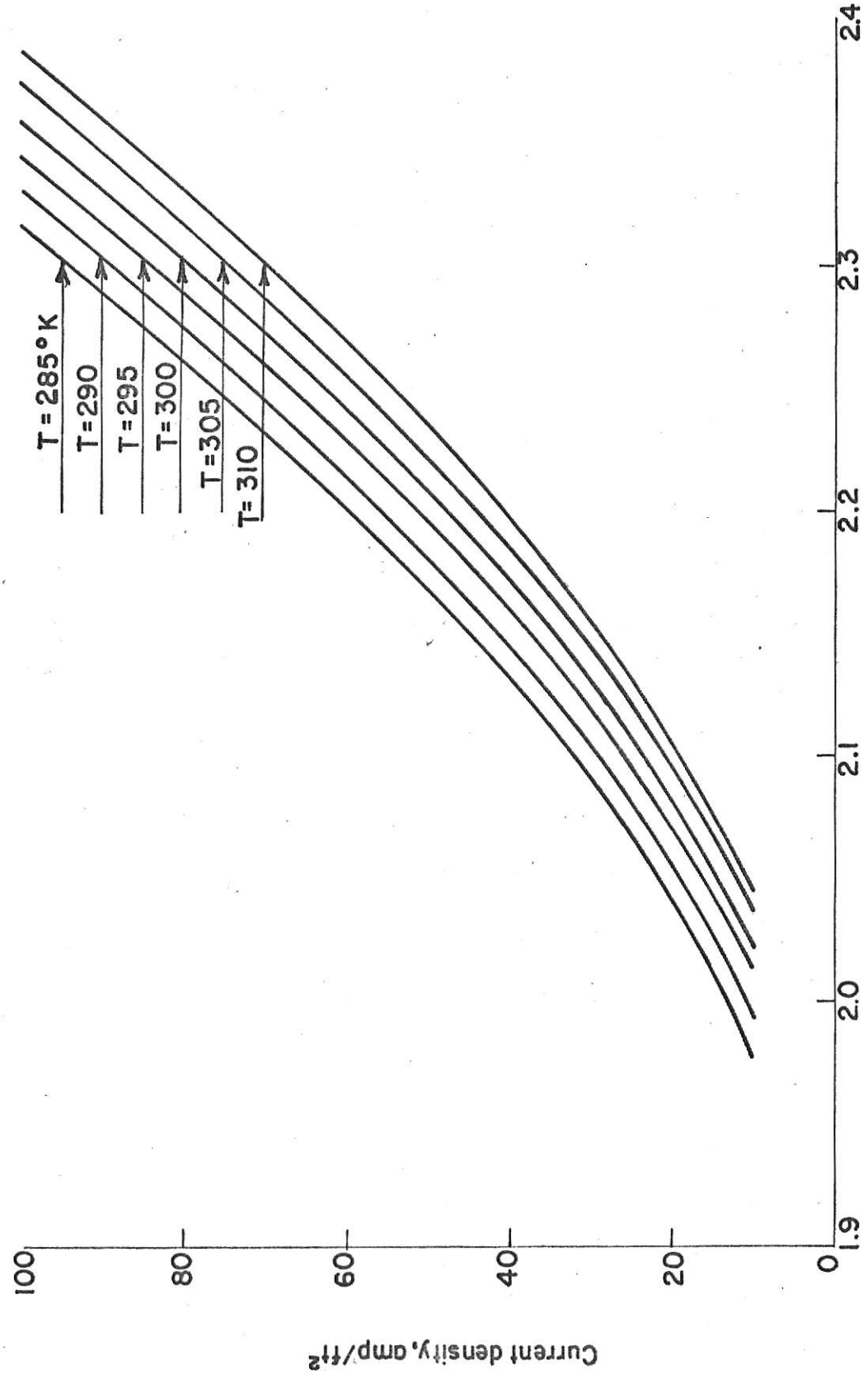

Fig. 3.2. Effect of temperature on voltage characteristics.

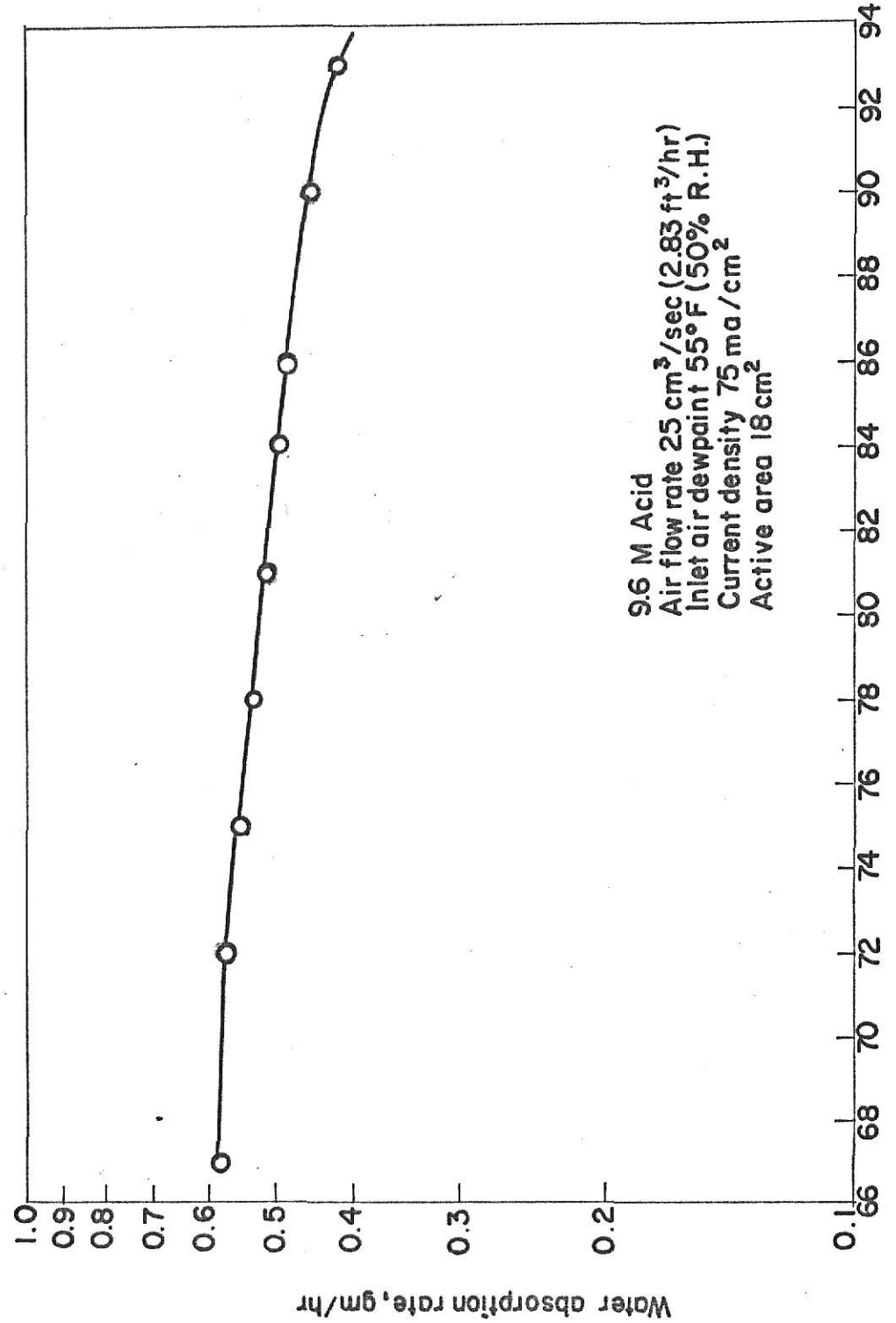

Fig.3.3. Water absorption variation with cell temperature [3.2].

of temperature and current density can be written as

$$W = 0.3 \left[I \times E + N \times 5.1 \times 10^{12} \frac{\mu' L}{A_c (b')^2} \left(\frac{m}{nF}\right)^{3.10} T^{0.75} i^{3.10} \right]$$

$$+ 0.62\ (N) + 3.02 + 0.03\ I \times (E - 1.48) \qquad (3.29)$$

with E given by equation (3.26). Equation (3.29) reduces to equation (3.13) at 75^{o}F. Substituting the expressions for N and E from equations (3.1) and (3.26) respectively, the total system weight can be written as

$$W = 0.3 \left[I \times (1.25 + 1.92 \times 10^{-3} T + 5.74 \times 10^{-4} T \log i + 0.002\ i) \right.$$

$$\left. + \frac{I}{A_e i} \times 5.1 \times 10^{12} \frac{\mu' L}{A_c (b')^2} \left(\frac{m}{nF}\right)^{3.10} T^{0.75} i^{3.10} \right]$$

$$+ 0.62 \left(\frac{I}{A_e i}\right) + 3.02 + 0.03\ I \times (1.25 + 1.92 \times 10^{-3} T$$

$$+ 5.74 \times 10^{-4} T \log i + 0.002\ i - 1.48) \qquad (3.30)$$

For the ARC module, the following data was taken from the report by Greenough et al [3.2].

$A_e = 0.0765\ ft^2$

$A_c = 14.5 \times 0.159/30\ ft^2$

$b' = 159/2.54$ mils

$L = 4.75/2.54$ in

The values of the other constants used in equation (3.30) are given below

$$m = 18/454 \text{ lbs.}; \quad n = 2 \frac{\text{equivalents}}{\text{mole}}; \quad F = 96{,}500 \frac{\text{coul}}{\text{equivalents}}$$

The total current required for a one man unit, I, to produce 2 lbs of oxygen per day, can be calculated by Faraday's law and the following two electrode reactions

anode: $2H_2O = O_2 + 4H^+ + 4e^-$

cathode: $4H^+ + 4e^- = 2H_2$

The value of I from the above reactions comes out to be 127 amp.

Substituting these numerical values in equation (3.30), the total system weight can be written as

$$W = 0.3 \left[127x\left(1.25 + 1.92x10^{-3}T + 5.74x10^{-4}T \log i + 0.002\, i\right)\right.$$

$$+ \frac{127}{0.0765} \times 5.1x10^{12} \times \frac{0.0182x4.75x30x(2.54)^2}{2.54x14.5x0.159x(159)^2} \times$$

$$\left(\frac{18}{454x2x96{,}500}\right)^{3.10} T^{0.75}\, i^{2.10} + 0.62 \left(\frac{127}{0.0765}\frac{1}{i}\right)$$

$$+ 3.02 + 0.03 \times 127 \times (1.25 + 1.92 \times 10^{-3} T$$

$$\left. + 5.74 \times 10^{-4} T \log i + 0.002\, i - 1.48\right)$$

or

$$W = 49.78 + 0.0805\ T + 0.085\ i + 1030\ i^{-1} + 0.024\ T \log i$$

$$+ 0.99 \times 10^{-8}\ T^{0.75}\ i^{2.10} \qquad (3.31)$$

Two special cases of weight optimization will now be considered. In case I, the weight will be minimized with respect to the current density only, keeping the temperature constant at $75^{o}F$. Case II is the more general case with temperature and current both varying continuously over specified limits.

Case I: WEIGHT MINIMIZATION WITH RESPECT TO CURRENT DENSITY

Substituting $T = 298^{o}K$ in equation (3.31), the total system weight expression reduces to

$$W = 83.78 + 0.085\ i + 7.15 \log i + 1030\ i^{-1} + 7.12 \times 10^{-7}\ i^{2.10} \qquad (3.32)$$

The current density which minimizes the total system weight can be obtained by differentiating the expression for W (equation 3.32) with respect to i and equating it to zero, i.e.,

$$\frac{dW}{di} = 0.0805 + \frac{7.15}{i} - 1030\ (i)^{-2} + 1.50 \times 10^{-6}\ (i)^{1.10} = 0$$

Solving the above equation the optimum current density can be obtained to be 76.5 amp/ft^2. It is unlikely, however, that the water-vapor electrolysis cell will be operated at this current density, because of the possibility of ozone formation at this current density. The total system weight has been plotted against the current density in Figure 3.4 and it can be seen here that there is little difference in the total

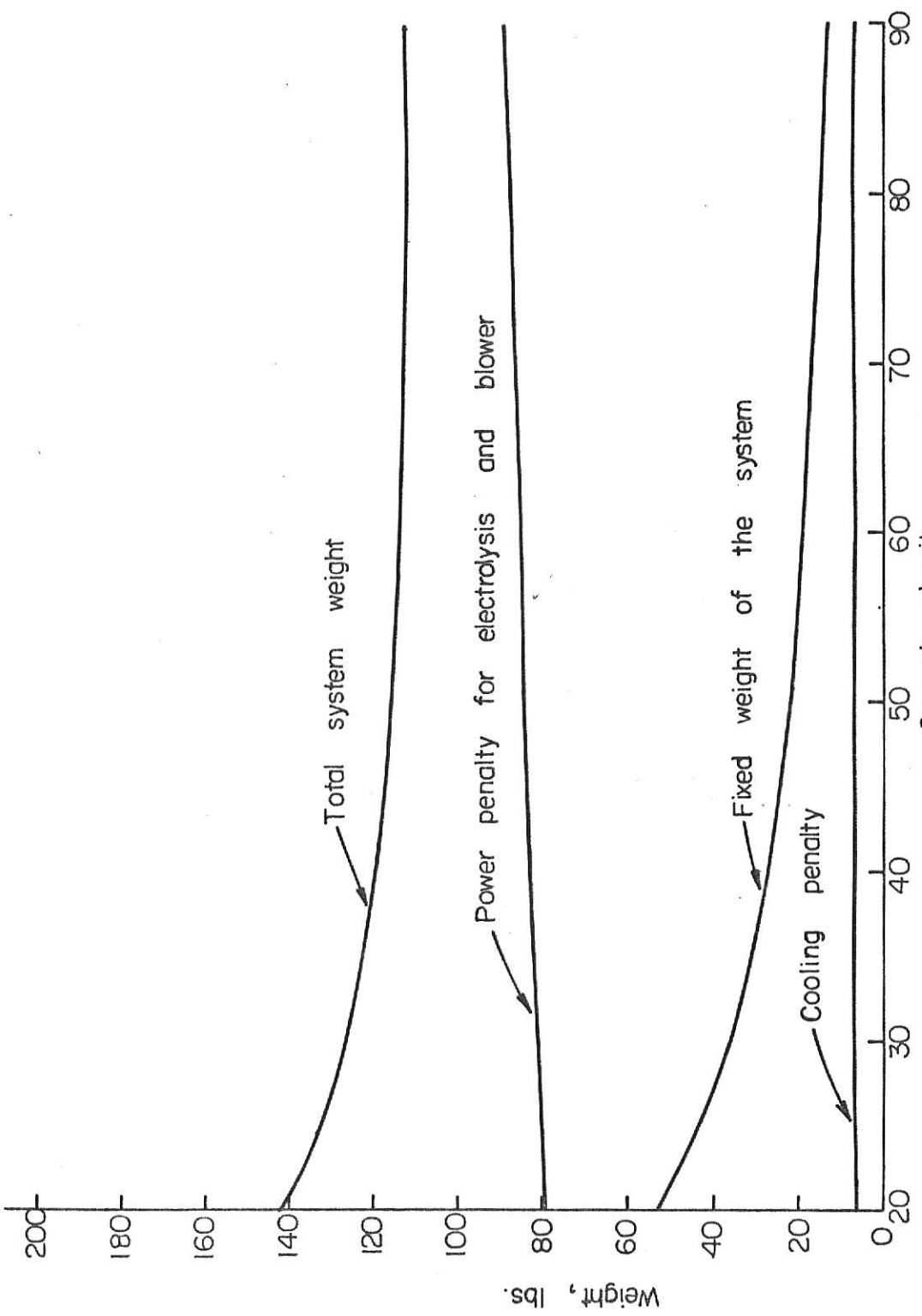

Fig. 3.4 Total system weight for the one man ARC module versus the current density.

system weight from 45 amp/ft^2 to 90 amp/ft^2.

Case II: WEIGHT MINIMIZATION WITH RESPECT TO CURRENT DENSITY AND TEMPERATURE

Equation (3.31) expresses the total system weight as a function of temperature and current density. A combination of these two variables can be found at which the total system weight is a minimum. Some constraints must be placed on the operating variables in order for the cell to function without side effects at these optimal operating conditions. The constraints that are placed on the temperature and the current density are

(i) The operating temperature should be between 20^{o}C and 60^{o}C, i.e. $293 \leq T \leq 333$.

(ii) The minimum limit on current density is 10 amp/ft^2 and the maximum limit is 50 amp/ft^2 (in order to prevent ozone formation) i.e., $10 \leq i \leq 50$.

The problem that has been stated above comes under the category of problems classified under the general heading of "Mathematical Programming" problems. A general statement of a problem of this type is "to find the maximum or minimum of a function when the variables are subject to equality or inequality constraints [3.16]". If the objective function and the constraints are linear it is called the "linear programming" and if they are nonlinear it is known as the "nonlinear programming". The differences in the various available methods for solving the nonlinear programming problems stem from the way the objective function is minimized and the way the constraints are incorporated. A short description of these methods is given in the book by Abadie [3.16]. Fiacco and

McCormick [3.7, 3.8, 3.9] developed a technique for solving the nonlinear programming problem which was based on an idea proposed by Caroll [3.13]. This technique uses a second order gradient method for function minimization and the weighted sum of the inverse of the constraints as the penalty function. The technique called the "sequential unconstrained minimization technique (SUMT) [3.7]" has been found to be more efficient and faster than other classical techniques. A brief description of the technique is given below.

Sequential Unconstrained Minimization Technique [3.7, 3.8, 3.9]

The general programming problem is to determine a vector $\bar{x}$ that minimizes $f(\bar{x})$ subject to $g_i(\bar{x}) \geq 0$, $i = 1, 2, \ldots, m$. The procedure for solving this problem is to define a function

$$P(\bar{x}, r_1) = f(\bar{x}) + r_1 \sum_{i=1}^{m} 1/g_i(\bar{x}) \tag{3.33}$$

where r_1 *is a positive constant.*

As a starting point for the process we determine $\bar{x}^o$ such that all the constraints are satisfied. From this point we proceed to a point $\bar{x}(r_1)$ that minimizes $P(\bar{x}, r_1)$ in the feasible domain. For this part we can employ any of the function minimization methods e.g. the simplex pattern search, the gradient and the conjugate gradient search, Hooke and Jeeves direct search etc. We now form a new function

$$P(\bar{x}, r_2) = f(\bar{x}) + r_2 \sum_{i=1}^{m} 1/g_i(\bar{x}) \quad \text{where} \quad 0 < r_2 < r_1$$

Starting from $\bar{x}(r_1)$ we find another point $\bar{x}(r_2)$ where $P(\bar{x}, r_2)$ is minimized. Continuing in this manner a sequence of points

$\{\bar{x}(r_k)\}$, k = 1, 2, ... are generated that respectively minimize $\{P(\bar{x}, r_k)\}$ where $\{r_k\}$ is a strictly monotonic decreasing sequence and $r_k \to 0$ as $k \to \infty$. It can be proved that under certain restrictions on $f(\bar{x})$ and $g_i(\bar{x})$ the sequence of P-minima, $\{P(\bar{x}, r_k)\}$, would converge to the optimum of the programming problem, i.e. $\bar{x}(r_k) \to \bar{x}_{min}$ and hence $f(\bar{x}(r_k)) \to f_{min}(\bar{x})$. The essential requirements on the function are the convexity of the P-function which, in turn, follows for f(x) convex and $g_i(x)$ concave.

A subroutine for the solution of the above mentioned problem was procured from Research Analysis Corporation [3.15]. The input to this subroutine package consists of three user supplied subroutines viz. RESTNT, GRAD1 and MATRIX and three information cards viz. the initial starting point card, the parameter card and an option card. A brief explanation of the user supplied subroutines and information cards, as they apply to the problem at hand, is given below [3.15]

Subroutine RESTNT (I, VAL)

When I = 0, this subroutine sets VAL = the value of the objective function (see equation (3.33)), i.e.

$$VAL = 49.78 + 0.0805\ T + 0.085\ i + 1030\ (i)^{-1} + 0.024\ T \log i$$

$$+ 0.99 \times 10^{-8}\ T^{0.75}\ i^{2.10}$$

When I = 1, 2, 3, 4 this subroutine sets VAL = the four constraints on the variables, i.e., depending upon whether I = 1, 2, 3, 4, VAL is set equal to T-293, i-10, 373-T, 50-i respectively.

Subroutine GRAD1(I)

When I = 0, this subroutine computes the values of the partial derivatives of the objective function with respect to the independent variables and sets them equal to DEL(J), i.e.

$$\frac{\partial W}{\partial T} = DEL(1) = 0.0805 + 0.024 \log i + 0.99 \times 0.75 \times 10^{-8} T^{-0.25} i^{2.10}$$

$$\frac{\partial W}{\partial i} = DEL(2) = 0.085 - 1030(i)^{-2} + \frac{0.024\ T}{i} + 0.99 \times 2.10 \times 10^{-8} T^{0.75} i^{1.10}$$

When I = 1, 2, 3, 4 the subroutine calculates the values of the partial derivatives of the constraints with respect to T and i and sets them equal to DEL(1) and DEL(2) respectively, i.e.

When I = 1

$$DEL(1) = \frac{\partial(T-293)}{\partial T} = 1$$

$$DEL(2) = \frac{\partial(T-293)}{\partial i} = 0$$

When I = 2

$$DEL(1) = \frac{\partial(i-10)}{\partial T} = 0$$

$$DEL(2) = \frac{\partial(i-10)}{\partial i} = 1$$

When I = 3

$$DEL(1) = \frac{\partial(373-T)}{\partial T} = -1$$

$$DEL(2) = \frac{\partial(373-T)}{\partial i} = 0$$

When I = 4

$$DEL(1) = \frac{\partial(50-i)}{\partial T} = 0$$

$$DEL(2) = \frac{\partial(50-i)}{\partial i} = -1$$

The gradients of the derivatives and the constraints are used in the second order gradient technique for function minimization.

Subroutine MATRIX(J)

When J = 0, this subroutine computes the upper triangular elements of the matrix of second partial derivatives of the objective function and sets them equal to A(I,J), i.e.

$$A(1,1) = \frac{\partial^2 W}{\partial T^2} = -0.99 \times 0.75 \times 0.25 \times 10^{-8}\ T^{-1.25}\ i^{2.10}$$

$$A(1,2) = \frac{\partial^2 W}{\partial i \partial T} = \frac{0.024}{i} + 0.99 \times 0.75 \times 2.10 \times 10^{-8}\ T^{-0.25}\ i^{1.10}$$

$$A(2,2) = \frac{\partial^2 W}{\partial i^2} = 2 \times 1030(i)^{-3} - 0.024\ T(i)^{-2} + 0.99 \times 2.10 \times 1.10 \times 10^{-8}\ T^{0.75}\ i^{0.10}$$

When $I \neq 0$, this subroutine computes the upper triangle elements of the matrix of the second partial derivatives of the constraints. These are all zero in the present case, because the constraints are linear.

These second partial derivatives are used in second order gradient technique of function minimization.

The input cards to the subroutine consist of the following, in the order given below

(i) Parameter Card. This supplies the values of EPSI, RHOIN, RATIO, TMMAX, M and N. The format is given in ref. [3.15] and the meaning of the symbols is explained below and the values used for the present problem is given in paranthesis.

EPSI. The tolerance used to decide if an unconstrained *minimization* has been reached (10^{-4}).

RHOIN. Initial value of r, the multiplier for the penalty function (10^{4}).

RATIO. Parameter used to compute consecutive values of r; $r_{i+1} = r_i/\text{RATIO}$ (4).

TMMAX. Maximum amount of time for solving problem, in seconds (180).

M. Number of nontrivial constraints (4).

N. Number of variables (2).

Initial Starting Point Card. This supplies the initial values of the temperature and the current density to be used. Several values of initial starting points were used to investigates its effect on the solution time.

Option Card. This enables one to choose from the several options available. A detailed description is given in the RAC supplied subroutine [3.15].

RESULTS AND DISCUSSION

The one dimensional weight minimization with respect to the current density only (Case I) shows that the current density which minimizes the total system weight is 76.5 amp/ft^2. It is, however, not possible to operate the cell at this current density because of ozone formation at values of current density higher than 50 amp/ft^2 [3.3]. The results have been plotted in Figure 3.4.

There is another variable which affects the total system weight, viz. the temperature. In case II, the temperature and the current density have been found which minimize the total system weight. The simulation of the total system weight in Figure 3.5 shows that the problem at hand is a convex programming problem and therefore the sequential unconstrained minimization technique can be applied. The shaded area in Figure 3.5 is the feasible domain i.e., the domain bounded by the constraints of the problem.

It can be seen from the simulation results that an unconstrained minima would be completely out of the range of the actual operating conditions for the water-vapor electrolysis. For the problem at hand, the current density is constrained to lie between 10 and 50 amp/ft^2 and the temperature between 300^{o}K and 340^{o}K. The maximum current density and the maximum temperature are dictated by the fact that above these values of temperature and current density there are side reactions in the cell, which reduce the efficiency of the cell. The minimum cell temperature was arbitrarily fixed at 300^{o}K, which is slightly higher than the room temperature. The minimum current density of 10 amp/ft^2 is chosen, because below this value the operation of the cell would become uneconomical.

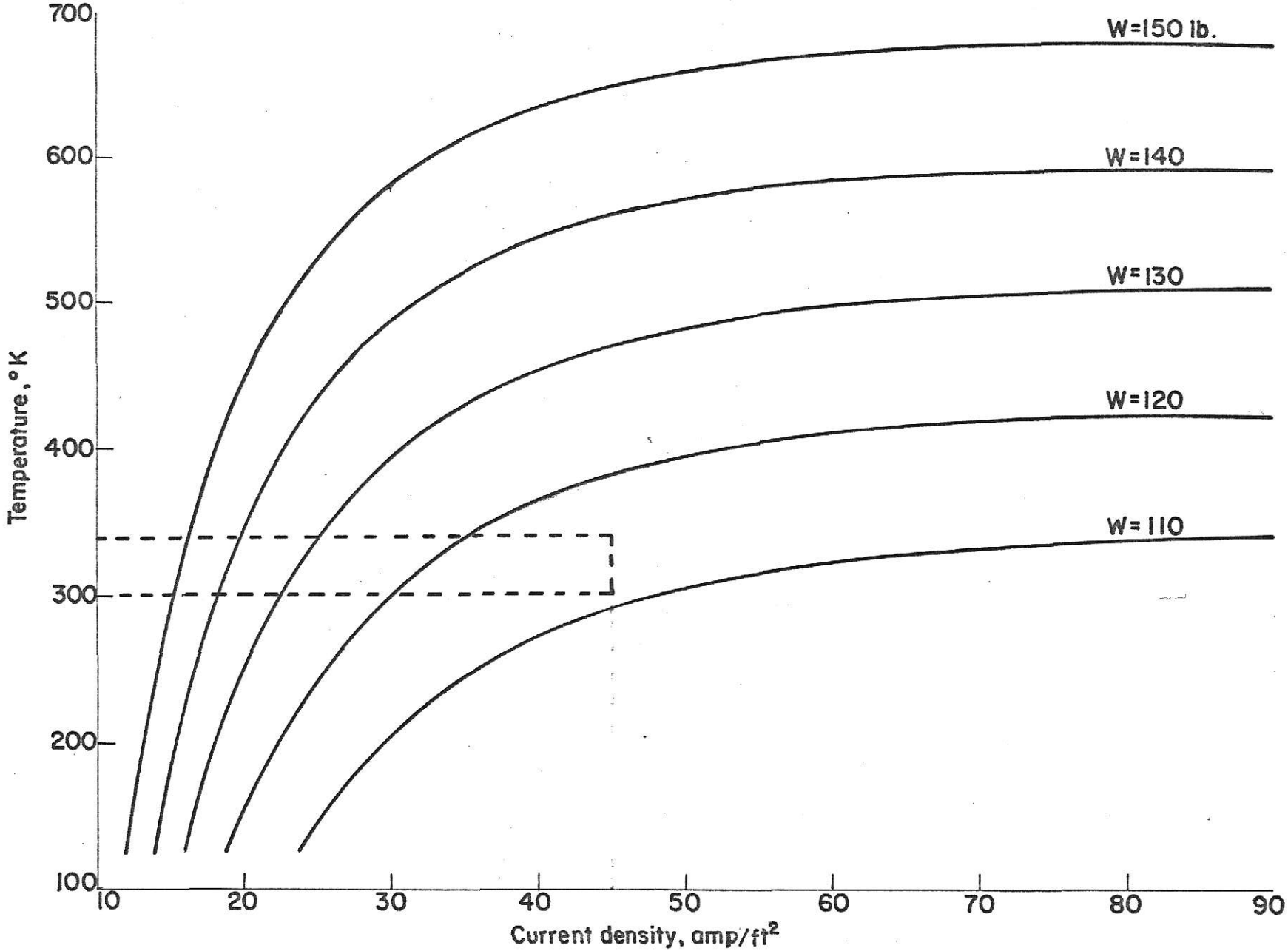

Fig.3.5. Simulation of total system weight as a function of temperature and current density.

Two starting points have been chosen for the first iteration. One is in the feasible domain while the other is outside this domain. Starting with the point in the non-feasible domain it has been found that the program immediately brings the point to the feasible domain by calling the subroutine FEAS. There is no significant loss of computational time as a result of the starting point being in the non-feasible domain.

Two different values of r have also been tried in order to investigate the effect this parameter has on the computational time. With the value of r set at 10,000 the execution time is 57 seconds. When the value of r is decreased to 300, the execution time increases to 70 seconds. A higher value of r is, therefore, favorable for a faster convergence.

The feasible region is shown in the enlarged scale in Figure 3.6 and the path of the solution is also shown there. The starting point for run number one is (350, 20) and the value of r for this run is 10,000. For run number two the starting point (300, 20) is within the feasible domain and the value of r is 300. It can be seen from Figure 3.6 that after a first few iterations, the solution path for the two runs coincide. It can also be noted that during the final stages the convergence is agonizingly slow. This is due to the fact that the gradient technique was used for minimization and this technique is very slow near the optimum of the problem. For making this technique work faster it is suggested that one should switch over to the Gauss method near the optimum.

The vlaues of the temperature and the current density that minimize the total system weight are $300^{o}K$ and 45 amp/ft^{2} which are at the boundary of the constraint region. The total system weight at these operating conditions is 110 lbs. It might be noted by looking at Figure 3.5 that

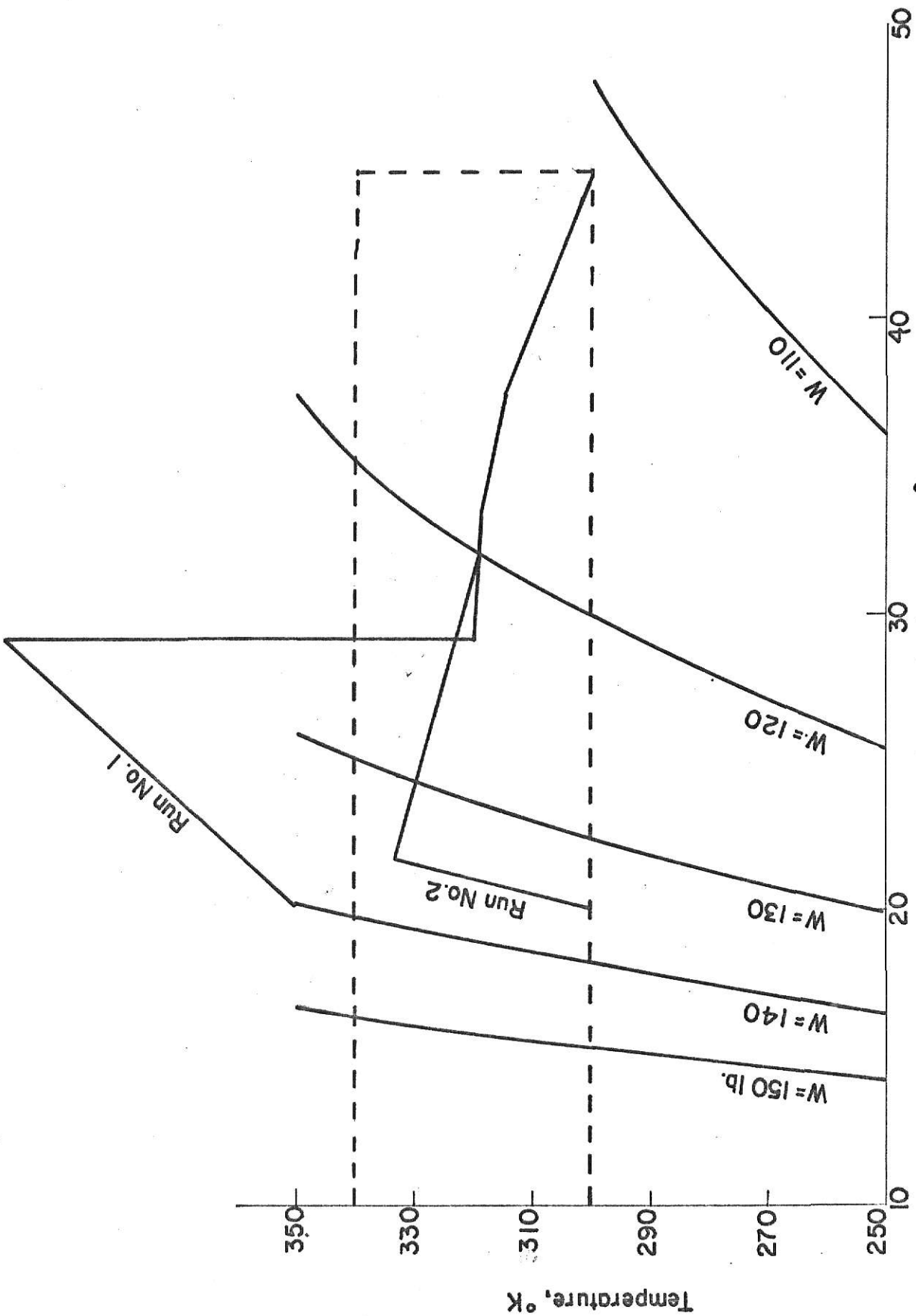

Fig. 3.6. Solution path for the various runs.

near the optimum point the contour lines are quite far apart, indicating that we have a very shallow minimum, therefore, the relative gain by changing the operating conditions near this point is relatively low.

CONCLUSION

In the present work an expression for the weight of the ARC module for generating a man's daily requirement of oxygen (2 lb/day) has been derived first as a function of current density. The current density for which the weight of the module is minimum has been shown to be 76.5 amp/ft^2. It has however been shown by the previous workers in this field that there is appreciable ozone formation at current densities above 50 amp/ft^2. This is due to the fact that the voltage characteristics of the cell are such that at current densities above 50 amp./ft^2, the cell voltage exceeds the voltage required for conversion of oxygen to ozone. The maximum current density under the above mentioned limitation is, therefore, approximately 50 amp./ft^2.

Temperature has been shown to be an important factor. It can affect the cell voltage characteristics and also the air properties like viscosity and density. The effect of temperature on voltage characteristics has been incorporated by dividing the total cell voltage into three parts, viz. the open circuit voltage, the chemical polarization and the ohmic polarization and the studying the effect of temperature on each theoretically. An expression for the total system weight has then been derived as a function of temperature and current density. It should be mentioned here that this is a purely theoretical expression and its validity against experimental observation has yet to be tested. As is the case with current density there are maximum and minimum limits on the temperature at which the cell can be operated. The problem is thus reduced

to minimizing a two dimensional nonlinear objective function with constraints on the variables. A simulation of the weight with respect to the temperature and current density shows that there is a very shallow minimum and the minimum is outside the constraint region. The two dimensional weight minimization was done by a nonlinear programming technique proposed by Fiacco and McCormick. The technique uses a second order gradient technique for function minimization and the weighted sum of the inverse of constraints as the penalty function. This technique has been found to be very effective for the weight minimization of the water-vapor electrolysis cell with constraints on temperature and current density. The results show that the temperature should be as low as possible and the current density as high as possible for the minimum weight of the cell. The cell module should therefore be placed in a cooler part of the space cabin, for example, near an air conditioner. A significant saving in the weight can also be achieved by having a cell which can operate at a lower cell voltage, since the penalty for electrolysis power, which is the product of cell voltage and current density, contributes much more that any other penalty to the total system weight.

SUMMARY

An expression for the weight of the water-vapor electrolysis cell has been derived as a function of temperature and current density. Operating temperature and current density have been found which minimize the total system weight by making use of the sequential unconstrained minimization technique. It has been shown that under the constraints imposed upon the variables, the temperature should be as low as possible and the current density as high as possible for a minimum in the system weight.

REFERENCES

3.1 Armstrong, R.C., et al., "Life Support System for Space Flights of Extended Durations." NASA CR-614 (1966).

3.2 Conner, W. J., B. M. Grenough, and G. M. Cook, "Design and Development of a Water-Vapor Electrolysis Unit," NASA CR-607 (1966).

3.3 Wydeven, T. and E. Smith, "Water-Vapor Electrolysis," Aerospace Medicine, 38 (10), 1045 (1967).

3.4 Wydeven, T. and R. W. Johnson, "Water-Electrolysis: Prospect for the Future," Transactions of ASME: Journal of Engineering for Industry, 531 (1968).

3.5 Clifford, J. E., A. C. Secrest, J. T. Gates, and C. L. Faust, "A Water Vapor Electrolysis Cell with Phosphoric Acid Electrolyte," NASA-CR 73170 (1966).

3.6 Clifford, J. E., B. C. Kim, and E. S. Kolic, "Study of a Water-Vapor Electrolysis Unit," Final Report for Ames Research Center & NASA, Contract No. NAS 2-2156, Feb. 1969.

3.7 Fiacco, A. V. and G. P. McCormick, "The Sequential Unconstrained Minimization Technique for Nonlinear Programming, a Primal-Dual Method," Management Science, 10 (2), 360 (1964).

3.8 Fiacco, A. V. and G. P. McCormick, "Computational Algorithm for the Sequential Unconstrained Minimization Technique for Nonlinear Programming," Management Science, 10 (4), 601 (1964).

3.9 Fiacco, A. V. and G. P. McCormick, "SUMT Without Parameters," Systems Research Memorandum, No. 121, Northwestern University, April 1965.

3.10 Knudsen, James G., Donald L. Katz, "Fluid Dynamics and Heat Transfer," Chapter 4, McGraw-Hill, 1958.

3.11 Smith, E. L. and T. Wydeven, private communication.

3.12 Perry, Joh H., "Chemical Engineer's Handbook," 4 ed., p 3-196, McGraw-Hill, New York, 1950.

3.13 Carroll, C. W., "The Created Response Surface Technique for Optimizing Nonlinear Restrained Systems", Operations Research, 9 (2), 169 (1961).

3.14 Glasstone, S., "Textbook of Physical Chemistry," 2 ed., p. 921, McGraw-Hill, New York, 1954.

3.15 McCormick, G. P., W. C. Mylander, III., and A. V. Fiacco, "RAC Computer Program for Implementing the Sequential Unconstrained Minimization Technique for Nonlinear Programming," SHARE No. 3189

NOMENCLATURE

a = a constant in the expression for chemical polarization

a_o = constant describing the variation of a with temperature

A_c = area of cross section for flow of air, ft^2

A_e = area of electrode, ft^2

b = a constant in the expression for chemical polarization

b_o = a constant describing the variation of b with temperature

b' = channel height of the absorption chamber

E = cell voltage, volts

ΔE_{chem} = chemical polarization, volts

E_o = open circuit voltage, volts

E_t = reversible cell voltage, volts

F = Faraday's number

$f(\bar{x})$ = objective function to be minimized by SUMT

ΔF^o = standard free energy change, $\frac{cal}{mole}$

$g_i(\bar{x})$ = constraint function

ΔH^o = standard enthalpy change, $\frac{kcal}{mole}$

i = current density, amp/ft^2

i_o = exchange current density, amp/ft^2

I = total current required for a one man unit, amp

K_p = equilibrium constant for the water dissociation

L = length of the flow path in absorption chamber, in

m = pound of water decomposed

n = number of equivalents per mole of water

N = total number of cells required for a one man unit

P_b = bank power for electrolysis, watts

P_f = power for driving the blower, watts

P_h = total heat to be removed from one man unit, watts

P_{H_2} = partial pressure of hydrogen in the cathode compartment, atm

P_{O_2} = partial pressure of oxygen in the anode compartment, atm

P_{H_2O} = vapor pressure of water over sulfuric acid, atm

$P(\bar{x},r_1)$ = modified objective function used in SUMT

ΔP = pressure drop in the absorption chamber, ps_i

q = air flow rate in the absorption chamber, ft^3/sec

q' = air flow rate in the absorption chamber, cm^3/sec

r_1 = a positive constant used in SUMT

r_{wa} = water absorption rate for the cell, lb/sec

r'_{wa} = water absorption rate for the cell, gm/hr

r_{ws} = theoretical rate of water electrolysis at a current density i, lb/sec

R = gas law constant, $\frac{cal}{mole\ ^oK}$

T = temperature of the cell, ^oK

v = average air velocity in the absorption chamber, ft/sec

W = total system weight of a one man unit, lb

W_b = fixed weight of the one man unit, lb

W_c = weight penalty for cooling, lb

W_E = weight penalty for electrical power consumed, lbs

$\bar{x}$ = vector of independent variables, x_1, x_2, ...

α = constant referred to as the transfer coefficient

μ = viscosity of air at temperature T, centipoise

μ' = viscosity of air at $75^{o}F$

CHAPTER 4

MODELING OF THE ABSORPTION CHAMBER

In this work a dispersion model for the absorption chamber is developed, and a nonlinear parameter estimation technique is used to estimate the parameters of the model using artificially generated data. In the water-vapor electrolysis cell, humid air is made to pass over a sulfuric acid-silica gel matrix in an absorption chamber (Figure 4.1) [4.2]. The water absorbed by the matrix is subsequently electrolysed to produce hydrogen and oxygen. In the constant current mode of operation, if the inlet humidity varies over a large range, the phenomena of "drying" or "flooding" are observed to occur. Drying of the matrix is evidenced by a decrease in Faradic efficiency for water electrolysis, which indicates that side reactions are occuring in the cell [4.2]. Flooding occurs at high inlet humidities and is evidenced by a loss of some electrolyte from the matrix. In order to prevent "drying" or "flooding" in the cell, the rate of absorption of water in the cell should be exactly equal to the rate of theoretical decomposition of water by electrolysis. To propose a satisfactory design of the cell, it is, therefore, necessary to have a model which can accurately describe the mass transfer characteristics of the cell.

Some attempts at modeling the absorption chamber of the water-vapor electrolysis cell were made by Engel [4.1] and Clifford et al. [4.2]. Both these workers have made use of transport equations involving mass, momentum and energy balances. In an electrolysis cell system where water is introduced into the electrolyte by passing humid air over an electrode in contact with the electrolyte, environmental conditions and electrolysis cell characteristics will influence the water transfer process. The driving force

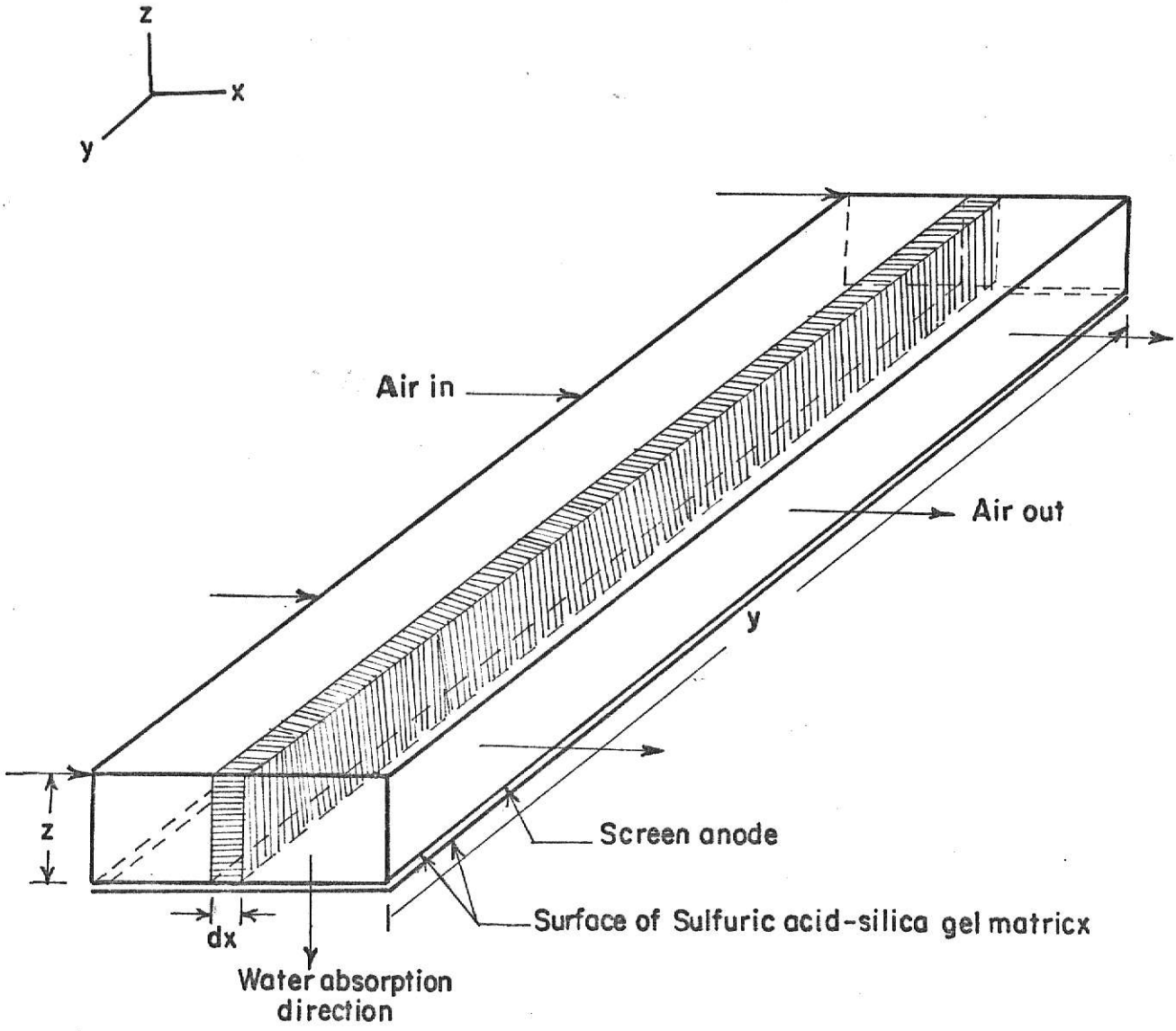

Fig.4.1. Absorption chamber of the Electrolysis cell.

for water absorption consists of the difference between the vapor pressure of the incoming air and the vapor pressure of the acid in the cell. The velocity of the air flowing over the electrode determines the rate at which water vapor is made available for absorption. Water transfer efficiency is a function of the flow pattern of air over the electrode surface and, therefore, is related to the geometry of the gas flow channel, the physical surface of the electrode, and the gas flow rate. Clifford [4.2] obtained some analytical solutions using arbitrarily imposed fully developed velocity profiles. Engel [4.1] proceeded under the assumption of laminar flow and attempted a numerical solution of the problem. Engel's approach, although it is more fundamental is rather unwieldy to work with. In the present attempt at modeling the system use has been made of the dispersion model. The reason for selecting the dispersion model is that the humidity profile along the length of the chamber affects the water absorption process. Since the height of the chamber is very small, changes in humidity with changes in height (z) may only be important near the anode. A one dimensional dispersion model which includes a mass transfer term to account for absorption at the anode may provide a simple and useful model which can account for the deviations from flow caused by the laminar velocity profile and other dispersion factors. The fitting of the dispersion model to the absorption chamber is much simpler than solving a set of coupled, nonlinear partial differential equations of heat mass and momentum transfer.

The fitting of any model to an actual system usually gives rise to a problem in parameter estimation. By comparing the results predicted by the model with those obtained by experimentation the parameter values are obtained which give the closest fit between the model and the actual situation.

The expression that is obtained by solving the dispersion model with the so called Danckwerts' boundary conditions is a nonlinear algebraic function with two unknown parameters. Marquardt's method [4.3] may be used to estimate the parameters in this model. The details of this method, which is one of the best available for such systems, are given in Appendix III. A computer program is available from the IBM SHARE library.

DEVELOPMENT OF A DISPERSION MODEL FOR THE ABSORPTION CHAMBER

Consider a differential element of the absorption chamber of volume yzdx (see Figure 4.1). A material balance at steady state for water for this element may be written as follows

$$\underset{\substack{\text{bulk}\\\text{flow}}}{(\text{In} - \text{Out})} + \underset{\substack{\text{axial}\\\text{dispersion}}}{(\text{In} - \text{Out})} - \text{loss by absorption} = 0$$

or

$$uA_c(C|_x - C|_{x+dx}) + DA_c\{\frac{dC}{dx}\Big|_{x+dx} - \frac{dC}{dx}\Big|_x\} - k\,y\,dx(C|_x - C_i\Big|_x) = 0 \qquad (4.1)$$

where

u = average velocity of air, ft/sec

A_c = area of cross section for flow, ft^2

C = Concentration of water vapor in air, $\frac{\text{lb of water}}{ft^3}$

D = dispersion coefficient, ft^2/sec

k = mass transfer coefficient for the absorption of water into the electrolyte matrix, ft/sec

C_i = concentration of water vapor in air at the air matrix interface. $\frac{\text{lb of water}}{ft^3}$

Dividing equation (4.1) by $uA_c dx$ and making use of the definition of a derivative, we have

$$-\frac{dC}{dx} + \frac{D}{u}\frac{d^2C}{dx^2} - \frac{ky}{uA_c}(C - C_i) = 0 \qquad (4.2)$$

Let us define two dimensionless variables H and η as follows

$$H = \frac{C - C_i}{C_0 - C_i} \qquad \text{and} \qquad \eta = \frac{x}{L} \tag{4.3}$$

where

C_0 = water vapor concentration at inlet, $\frac{\text{lb. of water}}{\text{ft}^3}$

L = length of the absorption chamber in the direction of flow, ft

Making use of these definitions equation (4.2) can be written as

$$\frac{D}{uL}\frac{d^2H}{d\eta^2} - \frac{dH}{d\eta} - \frac{kyL}{uA_c}H = 0$$

or

$$\frac{1}{Pe}\frac{d^2H}{d\eta^2} - \frac{dH}{d\eta} - B\,H = 0 \tag{4.4}$$

where

$Pe = \frac{uL}{D}$, the Peclet number

$B = \frac{kyL}{uA_c} = \frac{kL}{uz}$, a constant

For an isothermal absorption process, equation (4.4) may also be considered to be written in terms of dimensionless humidity, since at constant temperature a definition similar to equation (4.3) could be written using humidity in lb. of water/lb. of dry air as the dimensionless variable.

BOUNDARY CONDITIONS

A number of boundary conditions can be used for this model. For a detailed discussion of the various types of boundary conditions that can be used with the dispersion model, the reader is referred to papers by Fan and Ahn [4.4, 4.5]. One of the most often used set of boundary conditions is the

Danckwerts' boundary conditions. Validity of this set of boundary conditions has been re-examined from various points of views and approaches [4.6, 4.7, 4.8]. This set of boundary conditions has been used in the development below.

Danckwerts' boundary conditions can be mathematically stated in terms of dimensionless humidity as follows:

$$\begin{aligned} H - \frac{1}{Pe}\frac{dH}{d\eta} &= 1 \qquad \text{at } \eta = 0 \\ \frac{dH}{d\eta} &= 0 \qquad \text{at } \eta = 1 \end{aligned} \tag{4.5}$$

An analytical solution to equation (4.4) with the above set of boundary conditions can be found as follows [4.14]:

By the usual methods of solving second order ordinary differential equations we know that the solution will be of the form

$$H = A_1 e^{m_1 \eta} + A_2 e^{m_2 \eta} \tag{4.6}$$

where

$$m_1 = \frac{Pe}{2} + \frac{Pe}{2}\sqrt{1 + \frac{4B}{Pe}}$$

and

$$m_2 = \frac{Pe}{2} - \frac{Pe}{2}\sqrt{1 + \frac{4B}{Pe}}$$

A_1 and A_2 are arbitrary constants, which by the application of boundary conditions to equation (4.6) can be determined to be as follows:

$$A_1 = \frac{m_2 e^{m_2}}{m_2 e^{m_2}\left(1 - \frac{m_1}{Pe}\right) - m_1 e^{m_1}\left(1 - \frac{m_2}{Pe}\right)} \tag{4.7}$$

$$A_2 = \frac{-m_1 e^{m_1}}{m_2 e^{m_2}\left(1 - \frac{m_1}{Pe}\right) - m_1 e^{m_1}\left(1 - \frac{m_2}{Pe}\right)} \tag{4.8}$$

Equation (4.6) with the above expressions for m_1, m_2, A_1 and A_2 completely describes the dispersion model for the system. The only unknown parameters are Pe and B. The value of the Peclet number depends upon the flow properties of the system, which are described by the Reynolds number, and the fluid properties which are described by the Schmidt number. Correlations are available in the literature [4.9] which can predict the Peclet number, if the flow properties and the fluid properties are known. The higher the Peclet number, the closer is the system to the plug flow model. If Pe = ∞, it means that the system can be exactly described by the plug flow model. It should be noted, however, that this model is not the most appropriate one, if the flow behavior deviates considerably from plug flow. For the normal operation of the water-vapor electrolysis cell the Peclet number has been calculated to be about 10 (see Appendix IV).

The parameter B describes the mass transfer characteristics of the absorption chamber. It depends upon the geometry of the cell, as well as the absorption characteristics of the silica-gel sulfuric acid matrix. This in general will be a function of the temperature and the concentration of the acid in the matrix. In the present analysis, however, it will be assumed to be constant.

PARAMETER ESTIMATION BY MARQUARDT'S METHOD [4.3, 4.11]

Many techniques are available in the literature for estimating parameters. Their applicability and usefulness varies depending upon the type of model i.e., whether the model is differential or algebraic and whether it is linear or non-linear.

If the model is linear, then the parameters can be estimated easily by solving a set of simultaneous linear algebraic equations which are obtained by equating to zero the derivative of the squares of errors with respect to the parameters and then solving the resulting linear simultaneous equations.

If the model is non-linear then the equations that are obtained by differentiating the square of the error with respect to the parameters and, equating them to zero, are not linear. The parameter estimation in this case, therefore, is not as easy as in the linear case. Several techniques [4.10] like the Gauss method, steepest descent method, Marquardt's method, generalized Newton-Raphson method, Bard's method are, however, available for estimating parameters in such systems. These methods and a comparative discussion of them have been presented by Kowalic and Osborne [4.10].

Marquardt's method [4.3] is a combination of the Gauss and the steepest descent methods. It makes use of the steepest descent method during the initial iterations, when this method is more rapidly convergent and during the final iterations it switches over to the Gauss method. The Gauss method is characterized by rapid convergence, when sufficiently close to the final solution. The Gauss method is an iterative approach based upon the linearization of the non-linear function $f_i = f(\bar{x}_i, \bar{p})$ by a truncated Taylor series approximation about $\bar{p}_n$. The vector $\bar{p}_n$ represents the values of the parameters after the n^{th} iteration and $\bar{x}_i$ represents the vector of independent

variables at data point i. The expansion by the Taylor series gives

$$f(\bar{x}_i, \bar{p}_{n+1}) = f(\bar{x}_i, \bar{p}_n) + \sum_{j=1}^{P} \left(\frac{\partial f_i}{\partial p_j}\right) h_{j,n} \tag{4.9}$$

where

$$h_{j,n} = p_{j,n+1} - p_{j,n}$$

The objective function that is to be minimized now is given by

$$S = \sum_{i=1}^{N} [y_i - f(\bar{x}_i, \bar{p}_n) - \sum_{j=1}^{P} \left(\frac{\partial f_i}{\partial p_j}\right) h_{j,n}]^2 \tag{4.10}$$

where y_i = measured value of f at the i^{th} data point.

By setting the partial derivatives of S with respect to p_j equal to zero, we obtain

$$\frac{\partial S}{\partial p_j} = -2 \sum_{i=1}^{N} [y_i - f(\bar{x}_i, \bar{p}_n) - \sum_{k=1}^{P} \left(\frac{\partial f_i}{\partial p_k}\right) h_{k,n}] \frac{\partial f_i}{\partial p_j} = 0 \tag{4.11}$$

This gives us a set of P linear equations (j = 1, 2, ..., P) in P unknowns h_k, k = 1, 2, ..., P, which can be solved. The initial assumed values of the parameters are then changed by $h_{k,n}$ and the technique is applied again to the function obtained with this new set of values of the parameters. This is continued until the procedures converge as $h_{k,n}$ approaches zero.

In the steepest descent method movement from the current trial value is in the direction of the negative gradient of S. The steepest descent direction is given by the row vector

$$-[\left(\frac{\partial S}{\partial p_1}\right), \left(\frac{\partial S}{\partial p_2}\right), \ldots, \left(\frac{\partial S}{\partial p_P}\right)]/[\sum_{i=1}^{P} (\partial S/\partial p_i)^2]^{1/2}$$

Thus, in this method, a search is made in the direction of the negative

gradient of S, which is at right angles to the direction given by the Taylor series expansion [4.3]. The step size is chosen so as to give the minimum S in the direction of steepest descent.

In Marquardt's modification, an algorithm is devised in such a manner as to take advantage of the fast convergence of the steepest descent method in the early stages, and that of the Gauss method, in the vicinity of the minimum. The following characteristics are desirable for fast convergence

(i) The correction applied should be within 90° of the negative gradient of S.

(ii) As the search gets closer to the minimum, the correction vector should coincide with the correction vector predicted by the Taylor series expansion.

(iii) In addition to choosing the direction, the step size should be controlled so that there is rapid convergence with minimum oscillation.

In the algorithm developed by Marquardt the direction and the step size are controlled simultaneously. The validity of this approach is given in appendix III and for a detailed discussion the reader is referred to the paper by Marquardt [4.3].

GENERATION OF EXPERIMENTAL DATA

No experimental data could be found for the variation of humidity along the length of the absorption chamber. In order to show the capabilities of this parameter estimation technique, data have been generated by using arbitrary values of the parameters B and Pe. Error has been introduced in this experimental data by a random number generator. Several sets of experimental data have been the dispersion model approximates the

completely mixed chamber as the Pe approaches zero, and as Pe tends to infinity the model reduces to the plug flow model. Previous research has shown that the model is good for modeling small deviations from plug flow such as occur in the system considered here.

RESULTS AND DISCUSSION

The air flow required for the production of a man's daily requirement of oxygen by the Ames Research Center module is approximately 60 cu. ft./min. [4.12]. This corresponds to a Reynolds number of about 500, which is well within the laminar range. Using this value of Reynolds number and taking N_{Sc} = 0.60 for diffusion of water in air [4.13] the axial Peclet number is about 10 (See Appendix IV). The use of the dispersion model to describe the system is desirable since the departure from plug flow substantially affects the humidity profile as shown in Figure 4.2.

The concentration profiles for various values of Pe and B are shown in Figures 4.2, 4.3, and 4.4. To illustrate Marquardt's technique of parameter estimation, data was artificially generated by assuming some value of Pe and B and solving the dispersion model. A random error of zero mean and σ = 0.0001 was introduced into this. The subroutine deck supplied by IBM [4.11] was used to get back the assumed values of the parameters. The use of this subroutine package is explained in the IBM Share Program [4.11]. The subroutine package also provides some statistical information about the confidence limits of the parameters. A sample output has been shown in Appendix III.

It can be seen from the figures that as we increase Pe, the humidity profile becomes closer to that described by a plug flow model. Even at a value of Pe = 10 (which is the value during the normal operation of the

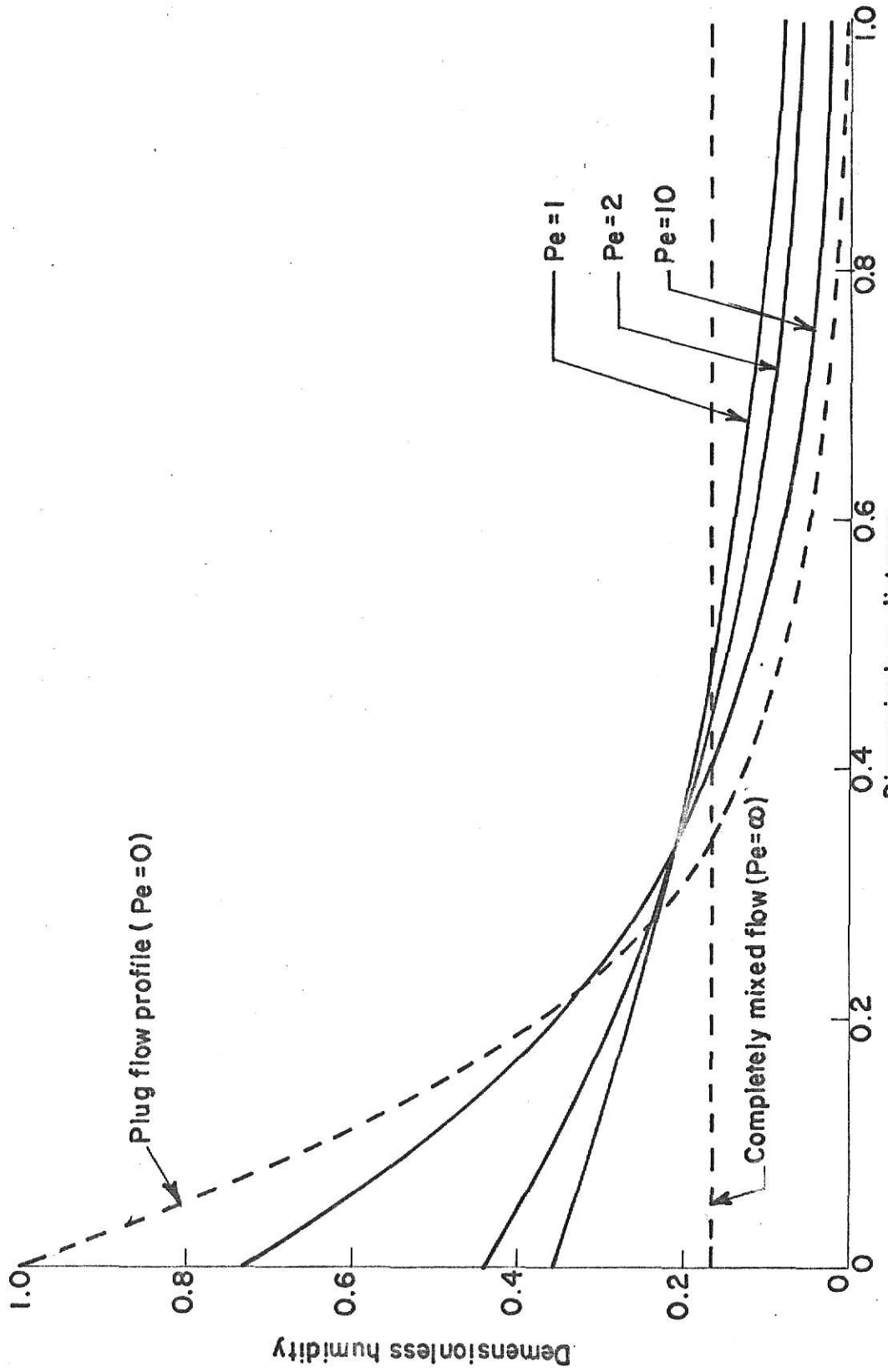

Fig.4.2. Variation of the humidity profile with Pe for B=5.

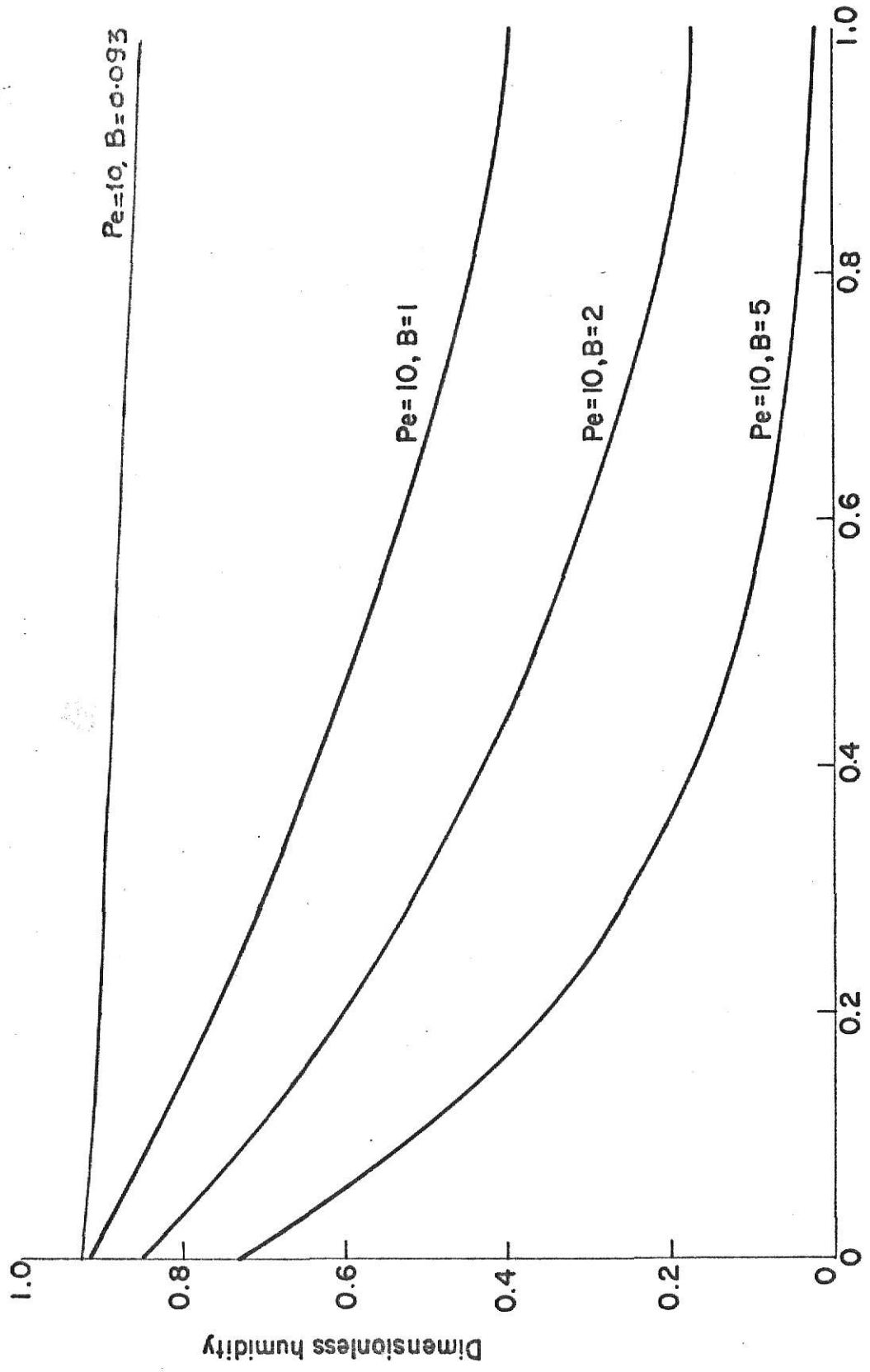

Fig.4.3 Variation of humidity profile with B for Pe=10.

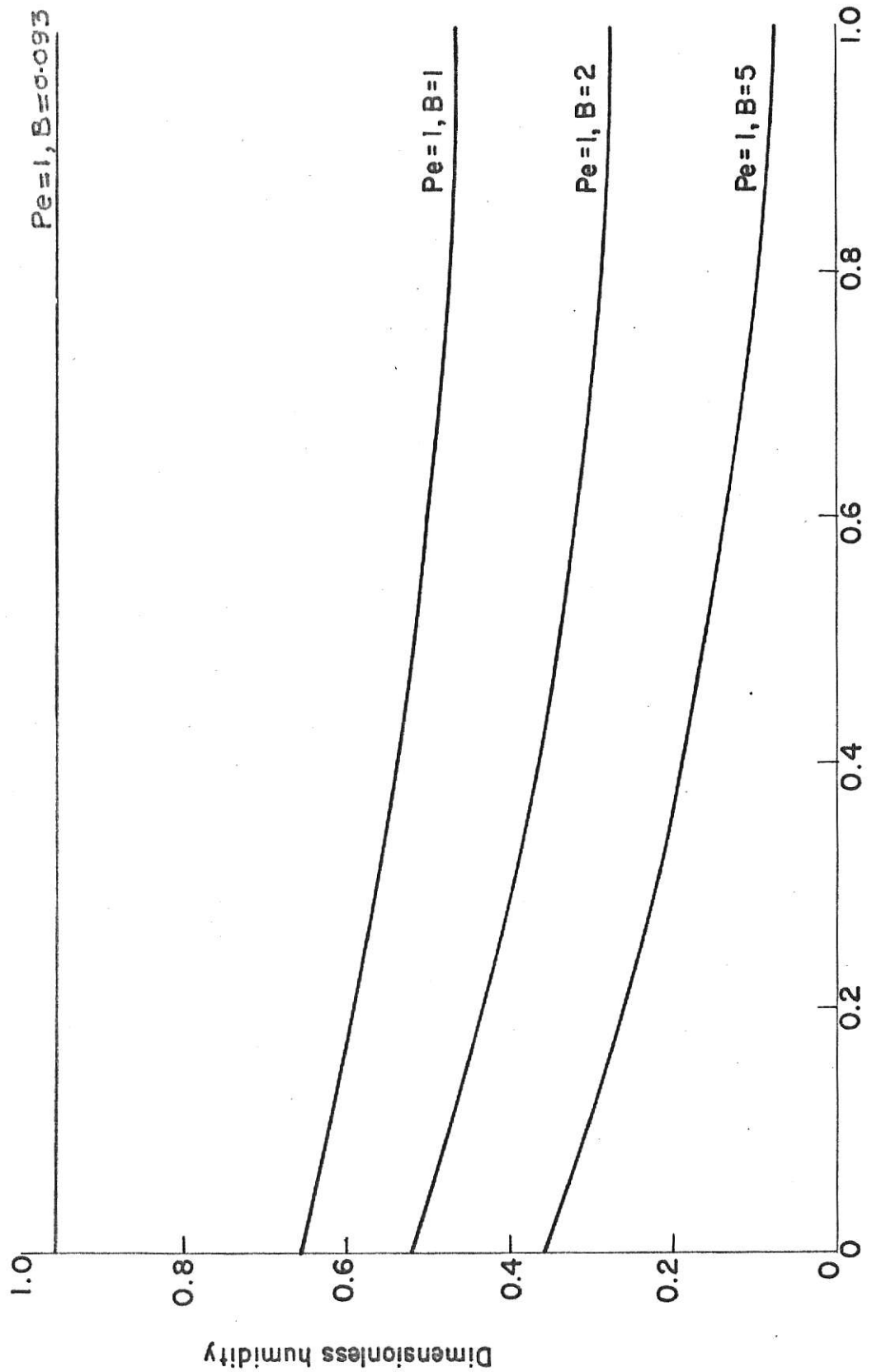

Fig.4.4. Variation of the humidity profile with B for Pe=1.

cell) the humidity profile is closer to that predicted by plug flow than that predicted by a completely mixed flow model. At a Reynolds number of 500 one would probably expect the behavior of the absorption chamber to be approximated by a completely mixed flow model. That this is not so, is clearly borne out by the above modeling scheme.

Figure 4.2 illustrates the magnitude of the deviations in the humidity profile that are experienced by using simplified models such as the plug flow or complete mixing models when the actual flow is according to dispersion model. However, accurate prediction of the quantity of water absorbed is probably of more interest than the exact shape of humidity profile. Table 4.2 compares results obtained using these three models for B = 1 and 5 (for modeling scheme. The humidity profile also depends upon the parameter B, which represents the absorption rate at the matrix surface. The only thing that B influences, significantly, however, is the exit concentration. The higher the value of B, the lower is the humidity of the air leaving the cabin. The value of $B = \frac{kyL}{uA_c}$ may be changed by varying the mass transfer coefficient or the velocity or the geometric dimensions of the cell.

Regarding the computational aspects of the method it can be said that it works very well in most cases. It was found that increasing the amount of normally distributed error decreases the accuracy of the parameter estimates quite significantly (See Table 4.1). The computation time and the number of iterations also increase with the measurement error. The computation time was also found to depend upon the initial estimates of the parameters.

One final remark should be made here regarding the number of parameters in the model. In the dispersion model there are actually two parameters B

Table 4.1. PARAMETER ESTIMATES FOR THE DISPERSION MODEL FOR DIFFERENT VALUES OF STANDARD DEVIATION

Standard deviation of measured data	Parameter	Assumed value	Recovered value	Standard error in parameter	No. of Iterations
$\sigma = 0.0$	B(1)	5.580×10^{-6}	5.580×10^{-6}	0.630×10^{-10}	3
	B(2)	10.916	10.916	0.124×10^{-3}	
	B(3)	0.916	0.916	0.265×10^{-7}	
	B(4)	-0.916	-0.916	0.111×10^{-6}	
$\sigma = 0.0001$	B(1)	5.580×10^{-6}	0.280×10^{-6}	0.857×10^{-7}	4
	B(2)	10.916	11.664	0.337	
	B(3)	0.916	0.916	0.657×10^{-4}	
	B(4)	-0.916	-0.915	0.267×10^{-3}	
$\sigma = 0.001$	B(1)	5.580×10^{-6}	0.787×10^{-9}	0.519×10^{-8}	49
	B(2)	10.916	18.076	0.729	
	B(3)	0.916	0.914	0.669×10^{-3}	
	B(4)	-0.916	-0.911	0.237×10^{-2}	

Table 4.2. PERCENT REDUCTION IN HUMIDITY AS PREDICTED BY DISPERSION PLUG FLOW, AND COMPLETE MIXING MODELS

	Percent reduction in humidity		
	$P_e = 0$ (Complete Mixing)	$P_r = 10$	$P_e \to \infty$ (Plug Flow)
B = 1	50	60	63.2
B = 5	83.3	97.6	99.4

and Pe. In the algebraic model that was obtained by solving the dispersion model using Danckwerts' boundary conditions there are four parameters (A_1, A_2, m_1 and m_2) which are functions of the original parameters B and Pe. In general, the lesser is the number of parameters, the more accurate is their estimate. In this case, however, reducing the number of parameters would have offset the increased amount of accuracy available by decreasing the number of parameters.

CONCLUSION

The dispersion model for the water transfer process in the absorption chamber of the water-vapor electrolysis cell has been developed. This model is much simpler than the models proposed by the previous workers in this field and yet, depending upon the estimates of the system parameters, it can describe the water transfer very precisely. The model can be very useful in designing a control system for the cell module. A technique for parameter estimation (Marquardt's method) has also been illustrated. This technique has been found to be very efficient for estimating parameters in nonlinear algebraic systems, like the one above. The IBM supplied subroutine package not only gives the estimate of the parameters but also much statistical information about the estimates. Since there was no experimental data available for the humidity profile in the absorption chamber of the water-vapor electrolysis cell, it was artificially generated by assuming some parameter values and then trying to recover those values. It has been found that if the standard deviation of the introduced error is less than 0.01%, the parameter values recovered are within ±1% of the assumed values. For greater values of standard deviations the recovered values were within ±10% of the assumed values.

SUMMARY

The absorption chamber of the water-vapor electrolysis cell has been represented by the dispersion model, which is much simpler and more adaptable to a control system analysis than the models considered by the previous workers. The parameters of the model have been estimated by a nonlinear parameter estimation technique known as Marquardt's method. The technique has been found to be very effective in estimating parameters of the above mentioned system.

REFERENCES

4.1 Engel, A. J., "Cycled Operation of Water Vapor Electrolysis Cell," private communication.

4.2 Clifford, J. E., et. al., "A Water Vapor Electrolysis Cell with Phosphoric Acid Electrolyte," NASA CR-771 (1967).

4.3 Marquardt, D. W., "An Algorithm for Least Square Estimation of Non-linear Parameters," J. Soc. Ind. Appl. Math., 2, 431 (1963).

4.4 Fan, L. T. and Ahn, Y. K., Digest of Joint Automatic Control Conference, Boulder, Colorado (1961).

4.5 Fan, L. T. and Ahn, Y. K., "Frequency Response of Tubular Flow System," Chem. Eng. Progr., Symposium Series, 46 (59), 91 (1963).

4.6 Ahn, Y. K., "A Diffusion Model of an Isothermal Tubular Flow Reactor," M.S. Thesis, Kansas State University, Manhattan, Kansas, 1962.

4.7 Fan, L. T. and Ahn, Y. K., I. E. C. Proc. Design and Devel., 1, 190 (1962).

4.8 Wehner, J. F. and Wilhelm, R. H., "Boundary Conditions of Flow Reactors," Chem. Eng. Sci. 6, 89 (1956).

4.9 Edwards, M. F. and J. F. Richardson, "Gas Dispersion in Packed Beds," Chem. Eng. Sci. 23, 109 (1968).

4.10 Kowalic, J. and M. R. Osborne, "Methods for Unconstrained Optimization Problems," American Elsevier, New York, 1968.

4.11 Marquardt, D. W., "Least Squares Estimation of Non-linear Parameters," IBM SHARE Program Library No. SDA 3094-01.

4.12 Clifford, J. E., Kim, B. C. and Kolic, E. S., "Study of a Water Vapor Electrolysis Unit," Final report for NASA Ames Research Center, Contract No. NAS 2-2156, Feb. 1969.

4.13 Perry, John H., "Chemical Engineers Handbook," 4 ed., p. 15-3, McGraw-Hill, New York, 1950.

4.14 Wylie, C. R., "Advanced Engineering Mathematics," 3 ed., p. 36, McGraw-Hill, New York, 1960.

NOMENCLATURE

A_c = area of cross section for flow, ft^2

B = a constant in the diffusion equation = $\frac{kyL}{uA_c}$

B(i=1,2,3,4) = four parameters that are estimated by Marquardt's method

C = concentration of water vapor in air, $\frac{lb\ of\ water}{ft^3}$

C_i = concentration of water vapor in air at the air matrix interface, $\frac{lb\ of\ water}{ft^3}$

C_o = inlet concentration of water vapor, $\frac{lb\ of\ water}{ft^3}$

D = diffusion coefficient, ft^2/sec

$f(\bar{x}_i,\bar{p})$ = function of variable $\bar{x}$ and parameter $\bar{p}$ that describes the nonlinear model

$h_{j,n}$ = difference in the j^{th} parameter values for the $(n+1)^{th}$ iteration and the n^{th} iteration

H = dimensionless concentration of water vapor

k = mass transfer coefficient for the absorption of water into the electrolyte matrix, ft/sec

L = total length of absorption chamber, ft

$p_{j,n}$ = value of the j^{th} parameter after the n^{th} iteration

P_e = peclet number = $\frac{uL}{D}$

S = objective function

u = average velocity of air, ft/sec

x = length in the flow direction , ft

y = width of the absorption chamber, ft

y_i = measured value of f at the i^{th} data point

z = channel height of the absorption chamber, ft

η = dimensionless distance in the x-direction

σ = standard deviation of introduced error

CHAPTER 5

IONIC TRANSPORT IN WATER-VAPOR ELECTROLYSIS CELL

Water-vapor electrolysis has been considered as a means of providing breathable oxygen for space missions of longer durations [5.1, 5.2]. A cell, with this purpose in mind was developed by the Ames Research Center of NASA and has been operated successfully for more than two thousand hours [5.3]. The cell operates by absorbing the moisture from the cabin air on a sulfuric acid-silica gel matrix and electrolyzing it subsequently to produce oxygen and hydrogen. The reason for using the solid-electrolyte matrix, instead of a liquid electrolyte, is that with the solid-electrolyte matrix a gas-liquid separation can be achieved even in zero gravity environments. Considerable trial and error has been previously used in the design and development of water-vapor electrolysis cells. The present work is an effort to develop a theoretical basis for cell design. Equations are presented which describe the transport of ions in solid-electrolyte matrices. After making some assumptions about the system the equations are solved analytically for the concentration distribution of hydrogen ions inside the matrix. A dimensionless parameter is identified that affects this distribution.

The electrolysis process is complicated because of the simultaneous occurrence of coupled, nonlinear transport of mass, momentum and energy in the presence of electrochemical reactions at the electrodes. The precise definition of these processes requires the statement and simultaneous solution of a set of coupled, nonlinear, partial differential equations. In view of the magnitude of the task of solving this set

of equations, one dimensional equations are used to describe the system. The approach is essentially that which has been outlined by Chapman [5.4] and Newman [5.5] for liquid electrolyte systems. The modifications are incorporated to take into account the fact that there is no bulk fluid motion but instead there is movement of fluid by capillary action. A model, which considers the matrix as a bundle of capillaries, is used. This type of model has been used for flow through porous media by Morel-Seytoux [5.6] and the physics and thermodynamics of capillary action in porous media has been discussed at length by Morrow [5.7]. The system is then identified with that of a minor ionic species in a well supported electrolyte [5.5]. This enables one to eliminate the potential term and the resulting differential equation is solved analytically to give the hydrogen ion concentration profile.

TRANSPORT EQUATIONS

The Nernst-Planck equation, which describes the flux of each dissolved species, is [5.5]

$$N_i = z_i U_i FC_i \nabla\phi - D_i \nabla C_i + C_i \bar{v} \tag{5.1}$$

where

N_i = flux of species i, moles/cm^2-sec

z_i = valence or charge number of species i

U_i = mobility of species i, cm^2-mole/Joule-sec

F = Faraday's constant, coul/equivalent

C_i = concentration of species i, moles/cm^3

ϕ = electrostatic potential, volts

D_i = diffusion coefficient of species i, cm^2/sec

$\bar{v}$ = fluid velocity, cm/sec

The three terms on the right hand side of equation (5.1) represent the three mechanisms of mass transfer [5.5]. The first term represents the motion of a charged particle in an electric field (the so called migration). The second term represents molecular diffusion due to a concentration gradient. The third term represents convection due to the bulk motion of the electrolyte.

For the case of an electrolyte which has been immobilized in a matrix, there is no bulk fluid motion and hence $\bar{v} = 0$. In a porous medium, whenever we have two immiscible fluids, there is another mechanism of mass transfer in operation [5.6]. If one of the two fluids preferentially wets the walls of the pores it can displace the other fluid without any external pressure gradient. The force that is responsible for this movement is the surface tension which acts at the interface of the two liquids. This motion of a

fluid into a capillary, thereby causing displacement of the prior occupant, is called imbibition with respect to the displacing fluid. For a detailed discussion of the flow of immiscible fluids in porous media the reader is referred to the articles by Morel-Seytoux and Morrow [5.6, 5.7]. In the water-vapor electrolysis cell we have a similar situation. The gases generated at the electrode and the liquid phase in which the ions move form the two immiscible phases. The silica gel matrix can be considered to be composed of a large number of capillary tubes of various sizes. For the purpose of modeling, however, these tubes have been considered to be of the same radii and of length equal to the distance between the electrodes [5.6, 5.7].

For the laminar motion of a fluid in a cylindrical capillary, we know that the average velocity is given by [5.8]

$$w = \frac{r^2}{8\mu} \frac{\Delta P}{L} \tag{5.2}$$

where r is the radius of the capillary tube, L the length of the capillary tube, ΔP the pressure drop across the tube, and μ the viscosity of the fluid.

If the movement of the fluid is caused by capillary forces, ΔP can be replaced by $2\gamma/r$ [5.6] where γ is the surface tension of the liquid. The expression for the average velocity in a capillary tube can, therefore, be written as

$$w = \frac{\gamma r}{4\mu L}$$

The molar flux of species i due to capillary motion is equal to $fC_i\bar{w}$, where f is the fraction of the matrix cross sectional area occupied by the capillary tubes.

Incorporating the flux due to capillary motion and removing the flux due to bulk motion, equation (5.1) can be written as

$$\bar{N}_i = - z_i U_i FC_i \nabla\phi - D_i \bar{\nabla} C_i + fC_i\bar{w} \tag{5.4}$$

where the magnitude of the vector $\bar{w}$ is given by equation (5.3).

Another important transport equation is the equation of continuity for each species [5.5]. This is essentially the statement of conservation of mass for any species and can be written as [5.5]

$$\frac{\partial C_i}{\partial t} + (\nabla \cdot \bar{N}_i) = R_i \tag{5.5}$$

Here R_i is the rate of production of species i (moles/cm^3-sec), in the bulk of the solution; however, in electrochemical systems the reaction is frequently restricted to electrode surfaces, in which case R_i is zero.

The current density i can be expressed as

$$i = F \Sigma z_i \bar{N}_i \tag{5.6}$$

where the summation is over all charged species that are carrying current.

Finally due to high mobility of species in electrolyte solutions under electric fields of magnitude ordinarily encountered, a state of electroneutrality holds for most of the bulk except in the double layer near the electrode. This can be written as

$$\Sigma z_i C_i = 0 \tag{5.7}$$

Equations (5.1), (5.5), (5.6) and (5.7) along with the appropriate boundary conditions and the expression for fluid velocity (the momentous transport equation) describe the transport processes in liquid electrolyte systems where the electrical potential field is known. For solid-electrolyte

matrix systems, equation (5.4) should be used instead of equation (5.1).

SOLUTION OF TRANSPORT EQUATIONS FOR SOLID ELECTROLYTE MATRIX SYSTEMS

Since there is no reaction in the bulk of the electrolyte, $R_i = 0$ and the equation of continuity for each species may be written as

$$\frac{\partial C_i}{\partial t} + (\nabla \cdot \bar{N}_i) = 0 \tag{5.8}$$

Substituting for N_i from equation (5.4) into equation (5.8), we have

$$\frac{\partial C_i}{\partial t} - D_i \nabla^2 C_i - z_i F \nabla(U_i C_i \nabla\phi) + \nabla(f C_i \bar{w}) = 0$$

If we restrict our attention to incompressible fluids ($\nabla \cdot \bar{w} = 0$), then the above equation may be written as

$$\frac{\partial C_i}{\partial t} - D_i \nabla^2 C_i - z_i F \nabla\cdot(U_i C_i \nabla\phi) + f\bar{w} \cdot \nabla C_i = 0 \tag{5.9}$$

The solution of equation (5.9) with the appropriate boundary conditions and along with equations (5.6) and (5.7) yields the concentration distribution within the electrolyte, if $\nabla\phi$ is known.

It appears that the complete solution of such a problem is a formidable task. Some limiting cases, however, can be considered. One limiting case is that of a binary electrolyte. For a binary electrolyte, equation (5.9) can be written as

$$\frac{\partial C}{\partial t} - D_+ \nabla^2 C - z_+ F U_+ \nabla\cdot C\nabla\phi + f \bar{w} \cdot \nabla C = 0 \tag{5.10}$$

$$\frac{\partial C}{\partial t} - D_- \nabla^2 C - z_- F U_- \nabla\cdot C\nabla\phi + f \bar{w} \cdot \nabla C = 0 \tag{5.11}$$

Here C is defined by

$$C = \frac{C_+}{\nu_+} \frac{C_-}{\nu_-} \tag{5.12}$$

where ν_+ and ν_- are respectively the numbers of anions and cations produced by the dissociation of one molecule of the electrolyte. Equation (5.12) is the direct result of the application of electroneutrality.

Subtracting equation (5.11) from equation (5.10), we have

$$(D_+ - D_-)\nabla^2 C + (z_+ U_+ - z_- U_-)F \nabla \cdot C\nabla\phi = 0 \tag{5.13}$$

Equation (5.13) can be used to eliminate $\nabla\phi$ either from equation (5.10) or from equation (5.11) to give

$$\frac{\partial C}{\partial t} + f \bar{w} \cdot \nabla C = D\nabla^2 C \tag{5.14}$$

where

$$D = \frac{Z_+U_+D_- - Z_-U_-D_+}{Z_+U_+ - Z_-U_-}$$

Equation (5.14) may be called the equation of "capilaric diffusion" by analogy with the equation of "convective diffusion" [5.5].

Another interesting limiting case is that of a minor ionic species in a "supporting" or "indifferent electrolyte" which increases the conductivity of the electrolyte and thereby reduces the electric field so that we may assume $\nabla\phi = 0$. In this case equation (5.9) reduces to

$$\frac{\partial C_i}{\partial t} + f \bar{w} \cdot \nabla C_i = D_i \nabla^2 C_i \tag{5.15}$$

This equation is similar in form to the convective diffusion equation.

APPLICATION TO WATER-VAPOR ELECTROLYSIS CELL

In the water-vapor electrolysis cell water is electrolyzed to give hydrogen and oxygen. The electrolyte is an 8M solution of sulfuric acid and is in the form of a matrix with silica gel. The sulfuric acid essentially reduces the field and increases the conductivity of the electrolyte solution. It does not take part in the electrolysis reaction as such. The electrode reactions for this cell are given below.

cathode:

$$4H^+ + 4e^- = 2H_2$$

anode:

$$2H_2O = O_2 + 4H^+ + 4e^-$$

The sulfuric acid can, therefore, be considered as a supporting electrolyte with the H^+ ions as the minor ionic species. Equation (5.15) is, therefore, applicable. Since the separation between the two electrodes in a water-vapor electrolysis cell is very small, the ions can essentially be considered to be in one dimensional movement from one electrode to the other. For the case of steady state one dimensional movement of H^+ ions equation (5.15) reduces to the following equation

$$f\, w \frac{\partial C_i}{\partial x} = D \frac{\partial^2 C_i}{\partial x^2} \tag{5.16}$$

Equation (5.16) can be solved to give the following expression for C_i

$$C_i = A_1 + A_2\, e^{\frac{fwx}{D}} \tag{5.17}$$

where A_1 and A_2 are arbitrary constants which can be determined by the application of the following boundary conditions.

At the anode the flux of H^+ ions should be related to the current

density. This condition can be mathematically stated as

$$z\,F\left(-D\,\frac{\partial C_i}{\partial x} + f\,C_i\,w\right) = i \qquad \text{at } x = 0 \tag{5.18}$$

Since the electrode reaction at the cathode is rapid, the hydrogen ion concentration at the cathode approaches zero; that is

$$C_i = 0 \qquad \text{at } x = L \tag{5.19}$$

Making use of equation (5.17) in the boundary condition, equations (5.18) and (5.19), the constants A_1 and A_2 can be determined to be

$$A_1 = \frac{i}{zFfw}$$

and

$$A_2 = -\frac{1}{e^{\frac{fwL}{D}}}\,\frac{i}{zFfw}$$

Substituting the expressions for A_1 and A_2 into equation (5.17) gives

$$C_i = \frac{i}{zFfw}\left[1 - \frac{e^{\frac{fwx}{D}}}{e^{\frac{fwL}{D}}}\right] \tag{5.20}$$

Equation (5.20) describes the H^+ ion concentration profile in the matrix of the water-vapor electrolysis cell. It is interesting to note the limit of C_i as w approaches zero. The limit can be calculated by the application of the l'Hospital's rule as follows:

$$\lim_{w\to 0} C_i = \lim_{w\to 0} -\frac{i}{zFf}\,\frac{\frac{f(x-L)}{D}\cdot e^{\frac{wf}{D}(x-L)}}{1}$$

$$= \frac{i\,(L-x)}{zFD}$$

This shows that for small values of w, C_i decreases linearly to zero as x goes from 0 to L.

Equation (5.20) can be made dimensionless by defining a reference concentration $C_r = \frac{i}{zFfw}$ and $\bar{C} = \frac{C_i}{C_r}$; $\bar{x} = \frac{x}{L}$ and $P = \frac{wL}{D}$.

The dimensionless concentration is then given by

$$\bar{C} = 1 - \frac{e^{fP\bar{x}}}{e^{fP}} \tag{5.21}$$

One of the main purposes of modeling is to define parameters, which are directly measurable and significantly affect the performance of the system.

RESULTS AND DISCUSSION

In any electrochemical system there are a host of processes going on at any time. The movement of ions is a net result of electrical forces, diffusion, capilaric motion, pressure variation, etc. The solution of transport equations is extremely difficult for such systems. For solid electrolyte matrices this difficulty is greatly magnified because of the complex geometry of the system. Because the detailed description of fluid flow in a porous medium is highly complicated, it appears reasonable to employ a simplified model which is approximately equivalent to the fluid flow in the actual medium. The "bundle of tube" model that has been used in our analysis of the H_2SO_4-silica gel matrix, water-vapor electrolysis cell seems to be a reasonable one for this system [5.5].

The test of a model lies in how well it can describe experimental results. The model should be able to identify parameters which may be measured and related to corresponding properties of the system. The objective has been achieved in this work by identifying a parameter fP. The variation of

concentration profile of hydrogen ions with fP is shown in Figure 5.1. The parameter fP is the product of the fraction of matrix cross sectional area occupied by the capillaries and the Peclet number for capillary motion. It can be seen that there is significant variation of the concentration profile with the parameter fP. The curves become more steep as the value of fP is increased. The steepness of the curve is an indication of the fact that most of the ions are concentrated near the cathode in a double layer. An extra amount of voltage, which is equal to the voltage of the concentration cell formed by this layer of ions and the cathode, is required. Therefore, in order to minimize the magnitude of concentration polarization in acid electrolyte cells, we should have as low a value of fP as possible. The low value of fP can be achieved by having a low value of f, the fraction of the total matrix cross sectional area occupied by the capillaries. It can also be achieved by having a low value of $P(=\frac{wL}{D})$, which means that we should have a small distance between the electrodes, a high value of diffusivity and a low value of w, the velocity of fluid in the capillary tubes. It should be noted here that concentration polarization has been found to be the largest contributor to the over voltage in acid electrolyte cells [5.9]. A reduction in concentration polarization could significantly affect the electrolysis power requirements and the weight penalty associated with it.

CONCLUSION

A model for ionic transport has been presented which can predict the concentration distribution of the hydrogen ions in the solid-electrolyte matrix of the water-vapor electrolysis cell. Using a bundle of capillary tubes model for the flow of electrolyte in the matrix, a parameter has been identified which affects this concentration distribution most significantly.

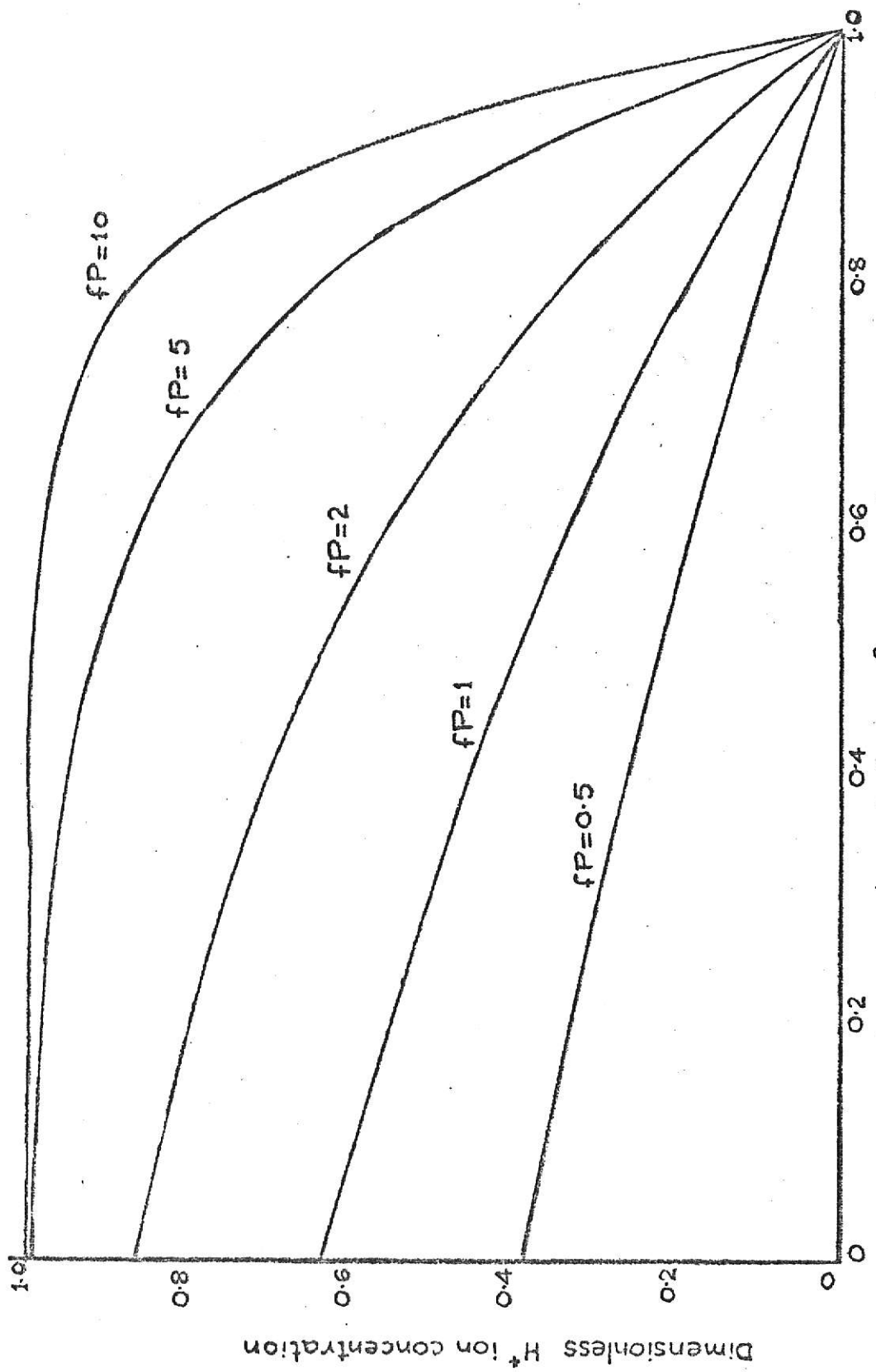

Fig 5.1. Variation of H^+ ion concentration profile with fP

It has been shown that by varying the value of this parameter the concentration distribution can be changed. This has a really significant implication. The concentration polarization, which is the largest contributor to the over voltage in the water-vapor electrolysis cell [5.9] is primarily dependent upon the concentration distribution of ions in the electrolyte. Where the electrolyte is in the form of a liquid, stirring of the liquid helps to reduce concentration gradients and hence the concentration polarization. For solid-electrolyte matrices, where stirring is not possible, the present approach indicates that the porosity of the matrix should be as low as possible for low values of concentration polarization. Although because of the assumptions involved, the approach of this work cannot be considered an exact representation of the transport processes taking place within the matrix, it does describe at least semi-quantitatively the effect of the matrix properties like porosity and the fluid properties like the viscosity (which affects the fluid velocity) on the concentration distribution of ions in the electrolysis cell.

SUMMARY

A model for the ionic transport in the water-vapor electrolysis cell has been developed. The model can predict the concentration distribution of the ions in the solid-electrolyte matrix. A parameter has been identified which affects this concentration distribution most significantly. Since concentration polarization depends upon the concentration distribution of the ions in the electrolyte, the approach indicates a way of reducing concentration polarization in cells using solid-electrolyte matrices.

REFERENCES

5.1 Wydeven, T. and R. W. Johnson, "Water Electrolysis: Prospect for the Future," Transactions of ASME: Journal of Engineering for Industry, 531 (1968).

5.2 Wydeven, T. and E. Smith, "Water-Vapor Electrolysis," Aerospace Medicine, 38 (10), 1045 (1967).

5.3 Clifford, J. E., B. C. Kim and E. S. Kolic, "Study of a Water-Vapor Electrolysis Unit," Final report prepared for the Ames Research Center of NASA (Feb. 1969).

5.4 Chapman, T. W., "Ionic Transport and Electrochemical Systems," AIChE Continuing Education Series, No. 4, p. 90, 1969.

5.5 Newman, J., "Transport Processes in Electrolytic Solutions," Advances in Electrochemistry and Electrochemical Engineering, vol. 5, (Eds., P. Delahay and C. W. Tobias), Interscience, New York, 1965.

5.6 Morel-Seytoux, H. J., "Introduction to Flow of Immiscible Liquids in Porous Media," Flow Through Porous Media, (Ed., J. M. De Wiest), Academic Press, New York, 1969.

5.7 Morrow, N. R., "Physics and Thermodynamics of Capillary Action in Porous Media," Ind. Eng. Chem., 62 (6), 32 (1970).

5.8 Bird, R. B., W. E. Stewart and E. N. Lightfoot, "Transport Phenomena," p. 46, John Wiley, New York, 1960.

5.9 Clifford, J. E. et al., "A Water-Vapor Electrolysis Cell with Phosphoric Acid Electrolyte," p. 38, NASA CR-771 (1968).

NOMENCLATURE

A_1, A_2	=	constants of integration
C_i	=	concentration of species i, moles/cm^3
D_i	=	diffusion coefficient of species i, cm^2/sec
F	=	Faraday's number
i	=	current density, amp/cm^2
L	=	length of the capillary tubes, also the distance between the electrodes, cm
N_i	=	flux of species i, moles/cm^2sec
r	=	radius of the capillary tubes, cm
R_i	=	rate of production of species i in the bulk of electrolyte, moles/cm^3sec
U_i	=	mobility of species i, cm^2mole/Joule sec
V	=	fluid velocity, cm/sec
w	=	velocity through the capillary tubes, cm/sec
z_i	=	valence or the charge number of species i
γ	=	surface tension of the electrolyte, dynes/cm
ϕ	=	electrostatic potential, volts
μ	=	viscosity of the liquid electrolyte

Chapter 6

RECOMMENDATIONS FOR FUTURE WORK

In the present thesis an attempt has been made to analyze theoretically the water-vapor electrolysis cell. Operating conditions have been defined at which the total cell system weight is minimum. To get a better understanding of the absorption process a model has been proposed for the absorption chamber. The discussion of the ionic transport in the cell has provided an insight into the design of such cells. There is, however, still a lot of work that needs to be done in order to get a better understanding of the cell and its reliable performance during spaceflights. The principle areas where research is needed have been indicated below.

(i) Since the cell is still in the advanced stages of development a lot of experimental work needs to be done, both in the areas of cell performance testing and obtaining data for theoretical analysis. One of the areas where the experimental data is required is the effect of temperature on the voltage characteristics of the cell. This will help in finding the operating temperature at which the system weight is minimum.

Since the absorption characteristics of the cell may also change with temperature, experiments should also be done to investigate this. In the dispersion model that has been presented in Chapter 4, the flow of air is assumed to be isothermal. This, then should be modified to take into account the effect of temperature.

(ii) One of the relatively unexplored areas is the integration of the water-vapor electrolysis cell with the rest of the life support system. The design of such an integrated life support system will

depend upon the interface considerations involving interaction with other specific subsystems in a direct manner (i.e., hydrogen delivery pressure, partial pressure of water vapor supplied to the electrolysis unit, voltage regulation of power supply) or an indirect manner (i.e., atmosphere contaminant control, thermal control, and humidity control [6,5]). For interface considerations the reader is referred to the report by Clifford [6.5]. The report by Kiraly and Babinsky [6.6] can be of considerable help in designing such an integrated life support systemp.

(iii) More work needs to be done in the areas of analyzing ionic transport in solid electrolyte matrices and redesigning the cell based on the guidelines provided by this theoretical analysis. Since the movement of ions through the liquid electrolyte is not the same as the flow through porous solid electrolyte matrices, it is suggested that the transport of ions through solid electrolyte matrices should be investigated in greater detail than has been done in Chapter 5. An explanation of the flow through porous media can be of considerable help and the papers by Morel-Seytoux [6.3] and Morrow [6.4] can be taken as the starting point for this type of study.

(iv) Another field in which a lot of work is possible is that of the design of a control system for the water-vapor electrolysis cell. Since the extreme conditions of humidities in the inlet air can produce "flooding" or "drying" of the cell [6.1,6.2] it is necessary to control variables like inlet air humidity, air flow rate, temperature of the air etc. For a safe and reliable performance of the cell, therefore, it is necessary to have an efficient control system along with it.

The design of a control system to control the humidity of a room by water-vapor electrolysis cell has been discussed in more detail below.

The purpose of the design is to maintain the water concentration inside the cabin at a predetermined desired value. This can be done by altering the cell voltage E, which in turn affects the electrolysis rate and hence the water concentration of the cabin.

The equation describing the rate of change of water concentration in the water-vapor electrolysis cell matrix is

$$Vf \frac{dC_M}{dt} = r_{wa} - r_{we} \tag{6.1}$$

where

V = total volume of the matrix, ft^3

f = fractional pore volume of the matrix

C_M = water vapor concentration in matrix $\frac{lb}{ft^3}$

r_{wa} = rate of water absorption over the matrix, lb/min

r_{we} = rate of water electrolysis, lb/min

Let us assume that the system is at steady state at $t = 0$ and define

$$\bar{C}_M = C_M - C_{Ms}$$

$$\bar{r}_{wa} = r_{wa} - r_{was}$$

$$\bar{r}_{we} = r_{we} - r_{wes}$$

where

C_{Ms} = steady state water vapor concentration in the matrix, lb/ft^3

r_{was} = rate of water absorption at steady state, lb/min

r_{wes} = rate of electrolysis at steady state, lb/min

At steady state, the material balance for the matrix gives

$$0 = r_{wa} - r_{we} \tag{6.2}$$

Subtracting equation (6.2) from (6.1) and writing in terms of deviation variables

$$Vf \frac{d\bar{C}_M}{dt} = \bar{r}_{wa} - \bar{r}_{we} \tag{6.3}$$

Taking Laplace transform on both sides of equation (6.3), we have

$$Vfs\ \bar{C}_M(s) = \bar{r}_{wa}(s) - \bar{r}_{we}(s)$$

or

$$\bar{C}_M(s) = \frac{\bar{r}_{wa}(s) - \bar{r}_{we}(s)}{Vfs} \tag{6.4}$$

The equation describing the rate of change of water concentration in the cabin is

$$V_R \frac{dC_R}{dt} = P_r - r_{wa} \tag{6.5}$$

where

V_R = volume of the cabin, ft^3

P_r = rate of water addition into the cabin by perspiration, lb/min

C_R = water concentration in the cabin, lb/ft^3

At steady state

$$0 = P_{rs} - r_{was} \tag{6.6}$$

Subtracting equation (6.6) from (6.5) and writing in terms of the deviation variables we have

$$V_R \frac{d\bar{C}_R}{dt} = \bar{P}_r - \bar{r}_{wa} \tag{6.7}$$

where

$$\bar{C}_R = C_R - C_{Rs}$$

and

$$\bar{P}_r = P_r - P_{rs}$$

Taking Laplace transform on both sides of equation (6.7) we have

$$V_R s\, \bar{C}_R(s) = \bar{P}_r(s) - \bar{r}_{wa}(s)$$

or

$$\bar{C}_R(s) = \frac{\bar{P}_r(s) - \bar{r}_{wa}(s)}{V_R s} \tag{6.8}$$

The rate of water absorption is given by

$$r_{wa} = kA\ (C_R - C_M) \tag{6.9}$$

The assumption here is that the water vapor concentration does not change along the flow path.

At steady state

$$r_{was} = kA\ (C_{Rs} - C_{Ms}) \tag{6.10}$$

Subtracting equation (6.10) from (6.9) we have

$$\bar{r}_{wa} = kA\ (\bar{C}_R - \bar{C}_M) \tag{6.11}$$

Taking Laplace transform on both sides of equation (6.11) we have

$$\bar{r}_{wa}(s) = kA\ (\bar{C}_R(s) - \bar{C}_M(s)) \tag{6.12}$$

The water electrolysis rate r_{we} is proportional to the current density through the cell as determined by Faraday's law, i.e.

$$r_{we} = Bi$$

where

B = constant of proportionality, $\frac{\text{lb/min}}{\text{amp/ft}^2}$

i = current density, amp/ft^2

or in terms of deviation Laplace variables we can write

$$\bar{r}_{we}(s) = Bi(s) \tag{6.13}$$

The current density i, in turn, is related to the cell voltage E, by the equation

$$i = \phi(E)$$

or in terms of Laplace variables we may write

$$i(s) = \Phi(E(s)) \tag{6.14}$$

Making use of equations (6.1) through (6.14) the block diagram shown in Figure 6.1 can be drawn. In Figure 6.1 the controller has been shown to be proportional. Integral and derivative modes can be added to it to have a better control. An analog simulation can be done using some numerical values and making use of Figure 6.1.

The above analysis should not be construed as complete in itself but should serve as a stepping stone for further research in this area.

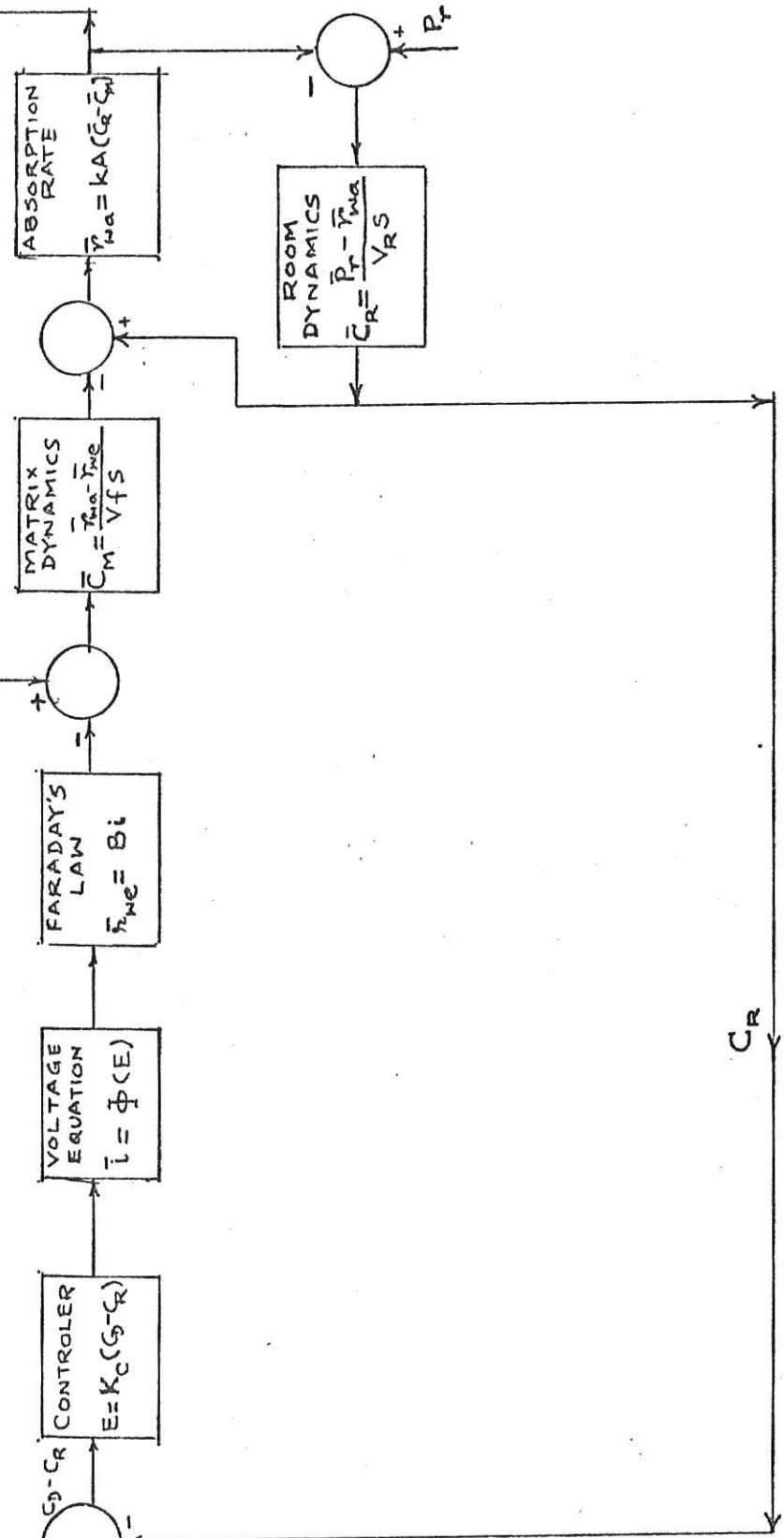

Fig. 6.1 Block diagram for controling the humidity of the cabin

REFERENCES

6.1 Wydeven, T. and R. W. Johnson, "Water Electrolysis: Prospect for the Future," Transactions of the ASME: Journal of Engineering for Industry, 531 (1968).

6.2 Conner, W. J., B. M. Greenough and G. M. Cook, "Design and Development of a Water-Vapor Electrolysis Unit," NASA CR-607 (1966).

6.3 Morel-Seytoux, H. J., "Introduction to the Flow of Immiscible Liquids in Porous Media," Flow Through Porous Media, (Ed. J. M. De Wiest), Academic Press, New York, 1969.

6.4 Morrow, N. R., "Physics and Thermodynamics of Capillary Action in Porous Media," Ind. Eng. Chem. 62 (6), 32 (1970).

6.5 Clifford, J. E., B. C. Kim and E. S. Kolic, "Study of a Water-Vapor Electrolysis Unit," Final Report prepared for Ames Research Center under Contract No. NAS 2-2156, 1969.

6.6 Kiraly, R. J. and A. D. Babinsky, "On-Board Aircraft Oxygen Generating System," NASA CR-73229 (1968).

Appendix I

SEQUENTIAL UNCONSTRAINED MINIMIZATION TECHNIQUE [1, 2]

The general programming problem is to determine a vector $\bar{x}$ that minimizes $f(\bar{x})$ subject to the constraints

$$g_i(\bar{x}) \geq 0 \qquad i = 1, 2, \ldots, m$$

Here $\bar{x} = (x_1, x_2, \ldots, x_n)^T$ is an n-dimensional column vector, where the subscript T denotes transposition.

C. W. Carrol [3] proposed a method for solving the above minimization problem which is based on the minimization of a new function

$$P(\bar{x}, r) = f(\bar{x}) + r \sum_{i=1}^{m} 1/g_i(\bar{x})$$

over a strictly monotonic decreasing sequence of r-values $\{r_k\}$. Under certain restrictions that will be reviewed subsequently, there exists a sequence of feasible points $\{\bar{x}(r_k)\}$ that respectively minimize $\{P(\bar{x}, r_k)\}$, and it follows that $\bar{x}(r_k) \to \bar{x}$ is a solution of the programming problem as $r_k \to 0$ $(k \to \infty)$. The following theorems and results will be needed to support the present development.

Define $R^0 = \{\bar{x} \mid g_i(\bar{x}) > 0, i = 1, \ldots, m\}$ and denote by R the closure of R^0.

Theorem 1: If

(1) R^0 is non-empty,

(2) $f(\bar{x})$ and $-g_i(\bar{x})$, i = 1, ..., m, are convex and twice continuously differentiable,

(3) for every finite k, is a bounded set,

(4) for every $r > 0$, $P(\bar{x}, r)$ is strictly convex, then:

(a) each function $P(\bar{x}, r_k)$ for $r_k > 0$ is minimized over R^0 at a unique $\bar{x}(r_k) \in R^0$, where

$$\nabla P[x(r_k), r_k] = \bar{0} \tag{1}$$

[where $\nabla = (\frac{\partial}{\partial x_1}, \frac{\partial}{\partial x_2}, \ldots, \frac{\partial}{\partial x_n})$]

(b) $\lim_{k\to\infty} P[\bar{x}(r_k, r_k)] = v_0$, where $v_0 = \min_{x\in R} f(x)$

Corollary 1: (a) $\lim_{k\to\infty} f[\bar{x}(r_k)] = v_0$,

(b) $\lim_{k\to\infty} r_k \sum_{i=1}^{m} 1/g_i[\bar{x}(r_k)] = 0$

A dual problem is associated with the above convex programming problem. The statement of the dual problem, which was originally given by Wolfe [4] is presented below

Dual problem:

Maximize

$$G(\bar{x}, \bar{u}) = f(\bar{x}) - \Sigma\, u_i g_i(\bar{x})$$

subject to

$$\nabla G(\bar{x}, \bar{u}) = \bar{0}, \qquad u_i \geq 0, \qquad i = 1, \ldots, m.$$

As a consequence of equation (1), the method yields a dual feasible point at each P minimum, where $u_i(r_k) = r_k/g_i^2[x(r_k)]$; $i = 1, \ldots, m$.

Theorem 2: Under the conditions of Theorem 1, the method yields dual feasible points $[\bar{x}(r_k), u(r_k)]$, and $\lim_{k\to\infty} G[\bar{x}(r_k), u(r_k)] = v_0$.

Since v_0 is the maximum value of $G(x, u)$ for dual feasible points, the following inequalities hold:

$$G[\bar{x}(r_k), \bar{u}(r_k)] \leq v_0 \leq f[\bar{x}(r_k)] \tag{2}$$

These bounds are of considerable practical importance in deciding when to terminate convergence.

Some of the important computational aspects of this method are described below.

Initial Value of r

It was observed that the number of iteration increases significantly if r is below a certain value or if it is above a certain value. The upper and lower limits on r are primarily dependent on the starting point $\bar{x}^0$. In order to reduce the number of iterations the following criterion can be applied to determine the value of r.

Criterion: One of the estimates of the amount by which $P(\bar{x}, n)$ exceeds its minimum value is the metrized magnitude of the gradient [5] given by

$$\nabla P(\bar{x}^0, r)^T \, [H_1 + rH_2]^{-1} \, \nabla P(x^0, r)/2 \tag{3}$$

where H_1 and H_2 are the Hessian matrices of $f(x)$ and $p(x) = \Sigma \, 1/g_i(x)$, respectively.

The value of r which minimizes the function given by (3) is an estimate of the value of r whose minimum P value is closest to that of $P(\bar{x}^0, r)$. If the H_1 matrix is assumed to be unimportant (which it is if the initial point x^0 is near several constraint boundaries), then

$$r_1 = \left(\frac{\nabla f(\bar{x}^0) H_2^{-1} \quad \nabla f(\bar{x}^0)}{\Delta p(x^0)^T \, H_2^{-1} \, p(x^0)}\right)^{1/2} \tag{4}$$

MINIMIZATION OF THE P FUNCTION BY GRADIENT METHOD

The principal techniques used to minimize P are the first and second order gradient methods. These are summarized below

$$x^2 = x^1 - \theta \nabla P(x^1) \tag{5}$$

and

$$x^2 = x^1 - \theta [\partial^2 P(x^1)/\partial x_i \partial x_j]^{-1} \nabla P(x^1) \tag{6}$$

In the first order gradient method, the second point, x^2, is obtained from the given starting point, x^1, by descending along the gradient of P, evaluated at the starting point, a distance proportional to θ. It can be shown that P must decrease if θ is taken small enough, the only alternative being that x^1 already minimizes P.

The second order method requires motion a distance (determined by θ) down the mapped gradient of P evaluated at x^1. The mapping is obtained by premultiplying the gradient of P by the inverse of the matrix of second partial derivatives of the P function. This procedure is based on approximation of P function using a Taylor's series expansion up through the second order terms, whereas the first order method is based on fitting a Taylor's series using only first order terms.

There are various strategies for selecting θ and these give rise to a wide variety of algorithms (see ref. [4]). A simple bracketing procedure has been used in the algorithm developed by Fiacco and McCormick. This works by systematically adjusting an initial arbitrary choice of θ by successive doubling or halving, until we approximately satisfy the orthogonality condition; that is, $\nabla P(x^1)^T \nabla P(x^2) = 0$.

Having thus determined x^2, $\nabla P(x^2)$ is computed, and the process is repeated until minimum has been approximated. When the first order gradient method is applied, the criterion used is the usual one that requires $|\nabla P(x^i, r)| < \varepsilon$, where ε is a small preassigned quantity and x^i is the accepted estimate of the

minimum. When the second order gradient method is used, a better criterion is to determine the convergence at x^i when

$$\frac{1}{2} \nabla P(x^i, r)^T H^{-1} \nabla P(x^i, r) < \varepsilon \tag{7}$$

where $\varepsilon > 0$, and H is the Hessian matrix of P evaluated at x^i.

Reduction of r

It was observed that

(i) it is highly advantageous to reduce r by a constant factor

(ii) the overall effort required to obtain a solution is relatively insensitive to the choice of factor, over a wide range of values of this factor.

Hence, our choice of r for the (i + 1)st minimization is given simply by $r_{i+1} = r_i/c$, where $c > 1$.

Final Convergence Criterion

Several criteria are possible. If the acceptable solution is within of the theoretical solution value, then the convergence criterion is to terminate when $r \Sigma 1/g_i[x(r)] < \varepsilon$. This is a result of the theory of duality discussed in section 1. The theoretical optimum value v_0 is bounded by the dual and primal function values, respectively G[x(r), u(r)] and f[x(r)]; that is

$$G[x(r), u(r)] \leq v_0 \leq f[x(r)] \tag{8}$$

Another way is to define a fractional error as the ratio of the absolute error to the solution value. The following inequalities then provide bounds on the fractional error in terms of known quantities:

(a) $G[x(r), u(r)] \leq v_0 \leq f(\bar{x})$ since the optimum value is bounded below by a dual feasible value, above by a primal feasible value;

(b) Assuming $f(\bar{x})$, v_0, and $G[x(r), u(r)]$ have the same sign, and $G[x(r), u(r)]$, $v_0 \neq 0$, then

$$f(\bar{x})/G[x(r), u(r)] \geq f(\bar{x})/v_0 \geq 1$$

(c) Rearranging (b) yields

$$(f(\bar{x}) - G[x(r), u(r)])/G[(x, r), u(r)] \geq (f(\bar{x}) - v_0)/v_0 \geq 0$$

the required bounds on the fractional error.

Summary of Computational Procedure

The following is a concise summary of the steps describing the computational algorithm:

1. Select a point x^0 interior to the feasible region. If such a point is not readily available repeated applications of the method itself can be used to obtain it.
2. Select r_1, the initial value of r.
3. Determine the minimum of $P(x, r_k)$ for current value of r_k.
4. If $k > 1$, estimate solution using extrapolation formula.
5. Terminate computations, if final convergence criteria are satisfied.
6. Select $r_{k+1} = r_k/c$ where $c > 1$.
7. If $k > 1$, estimate minimum for reduced r-value, using extrapolation formula. Continue procedure from step (3).

REFERENCES

1. Fiacco, A. V. and G. P. McCormick, "Computational Algorithm for the Sequential Unconstrained Minimization Technique for Nonlinear Programming," Management Science, 10 (4), 601 (1964).

2. Fiacco, A. V. and G. P. McCormick, "The Sequential Unconstrained Minimization Technique for Nonlinear Programming, a Primal-Dual Method," Management Science, 10(2), 360 (1964).

3. Carroll, C. W., "The Created Response Surface Technique for Optimizing Nonlinear Restrained Systems," Operations Research, 9 (2), 169 (1961).

4. Wolfe, P., "A Duality Theorem for Nonlinear Programming." Quarterly of Applied Mathematics, 13 (3), (1961).

5. Davidon, William C., "Variable Metric Method for Minimization," Argonne Nation Laboratory, Chicago, 1959.

Appendix II

WATER ABSORPTION RATE AS A FUNCTION OF HUMIDITY DRIVING FORCE

The rate of water absorption can also be represented by

$$r_{wa} = k\, A_e\, \Delta C_{\ell m}$$

where

r_{wa} = rate of water absorption, gm/sec

A_e = active area of electrode, cm^2

$\Delta C_{\ell m}$ = log mean driving force, gm/cm^3

k = rate constant for absorption, cm/sec

The log mean driving force is defined by

$$\Delta C_{\ell m} = \frac{(\Delta C)_{inlet} - (\Delta C)_{outlet}}{\ell m \frac{\Delta C_{inlet}}{\Delta C_{outlet}}}$$

In order to calculate the rate constant, k, we should first construct a graph of $\Delta C_{\ell m}$ vs. r_{wa}. The concentration of water vapor at the outlet can be calculated from Figure 3.1 by making an overall mass balance on the water, which gives

$$q\, C_{in} = r_{wa} + q\, C_{out} \qquad (2)$$

where

q in flow rate of air, cm^3/sec

C_{in}, C_{out} = concentration of water vapor in the air at the inlet and the outlet respectively, gm/cm^3

r_{wa} = rate of absorption of water, gm/sec

From the data of Figure 3.1, at each value of the inlet air humidity, we can calculate C_{in} and C_{out} and then we can construct a graph of $\Delta C_{\ell m}$ vs/ r_{wa}. The results of the calculation are shown in Table 1. The slope can be determined from Figure 1.

$$\text{slope} = k A_e = 0.049 \times 10^6 \text{ cm}^3/\text{hr}$$

$$k = \frac{0.049 \times 10^6}{18} \text{ cm/hr}$$

$$= 2.82 \times 10^3 \text{ cm/hr}$$

To obtain the value of r_{wa} for a cell of area 90 cm^2, we have to solve the following two equations simultaneously

$$27 \times 11.42 \times 10^6 = \frac{r_{wa}}{3600} + 27 \times C_{out}$$

$$r_{wa} = 2.82 \times 10^3 \times 90 \times \frac{(11.42-4.40) \times 10^{-6} - (C_{out}-4.40) \times 10^{-6}}{\ell m \frac{11.42 - 4.40}{C_{out} - 4.40}}$$

By trial and error, the following solution was obtained

$$r_{wa} = 0.634 \text{ gm/hr}$$

$$C_{out} = 4.92 \times 10^{-6}$$

By using the empirical formula proposed by Conner, the absorption rate for a cell with electrode area of 90 cm^2 can be calculated as follows

$$r_{wa} = 0.0621 \, q^{0.644}$$

We have at q = 27 cm^3/sec

$$r_{wa} = 0.0621 \, (27)^{0.644} = 0.518 \text{ gm/hr}$$

Table 1. Results of Calculations Made from Figure 3.1.

Inlet humidity hi, %	C_{in}, gm/cm^3	C_{out}, gm/cm^3	$\Delta C_{\ell m}$, gm/cm^3	r_{wa}, gm/hr
30%	6.78×10^{-6}	4.77×10^{-6}	1.08×10^{-6}	0.19
40%	8.69×10^{-6}	5.50×10^{-6}	2.34×10^{-6}	0.31
50%	11.42×10^{-6}	6.9×10^{-6}	4.39×10^{-6}	0.46
60%	13.21×10^{-6}	7.24×10^{-6}	5.27×10^{-6}	0.58

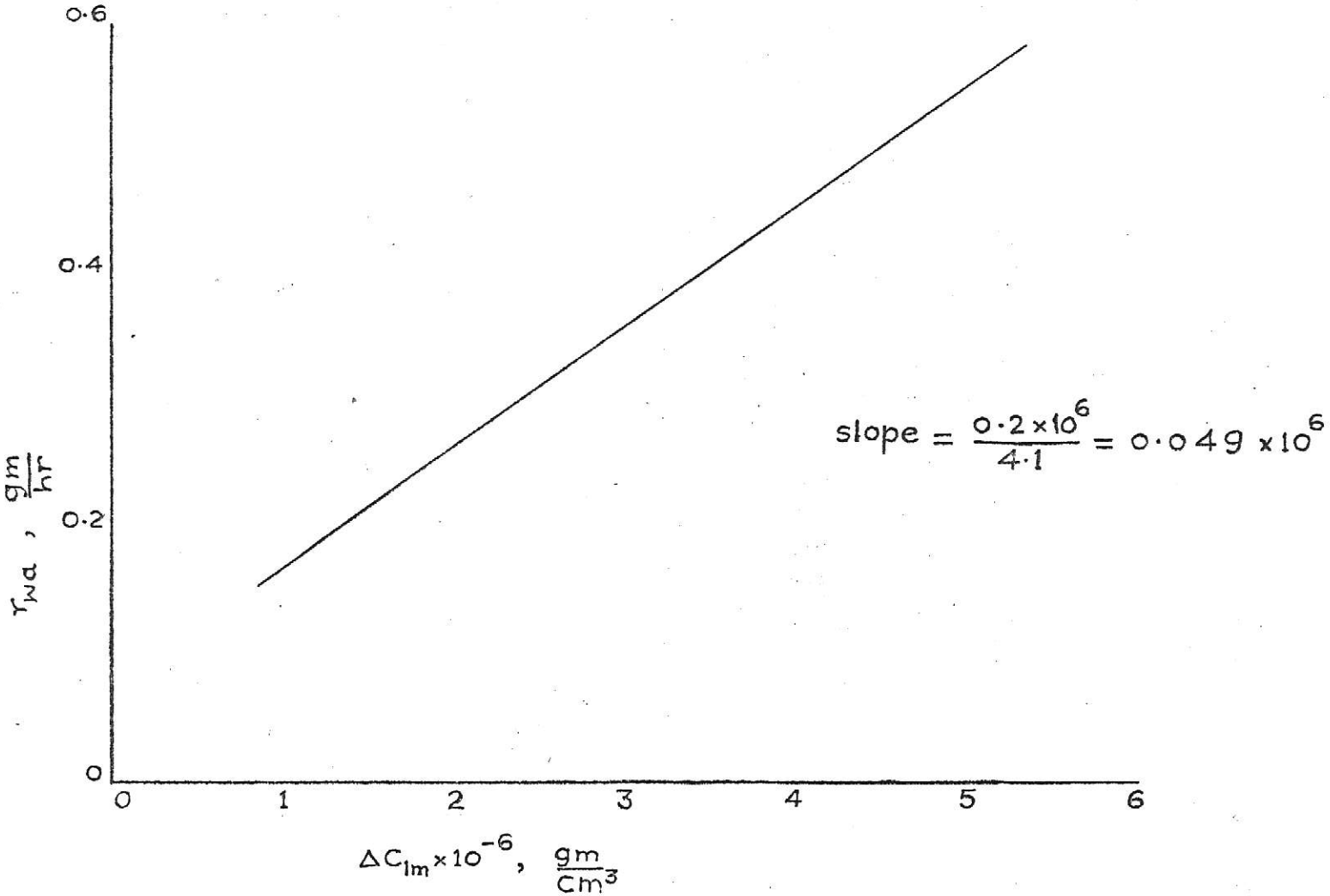

Fig. II-1 Absorption rate variation with the log mean water vapor concentration driving force

We see that the rates calculated by the two methods are not too different. The differences will increase, however, if the flow rate is changed from 27 cm^3/sec.

The value of the mass transfer coefficient, k, will approximately be the same for the ARC module as we have a similar situation there. Using this value of mass transfer coefficient and the dimensions of the ARC module, the value of parameter, B used in Chapter 4 can be calculated as follows.

The dimensions of the cell module are as follows

$L = 4.75$ cm

$\bar{z} = 0.159$ cm

The velocity of air, u, thru the absorption chamber during the normal operation of the cell is 8.4 ft/sec.

Therefore,

$$B = \frac{kL}{u\bar{z}} = \frac{2.82 \times 10^3 \times 4.75}{8.4 \times 30 \times 60 \times 60 \times 0.159}$$

$$= 0.093$$

Appendix III

NONLINEAR PARAMETER ESTIMATION BY MARQUARDT'S METHOD [1,2]

Many techniques are available in the literature for estimating parameters [3]. Their applicability and usefulness varies depending upon the type of model i.e., whether the model is differential or algebraic and whether it is linear or nonlinear. Marquardt's method is a nonlinear parameter estimation technique which makes use of the Gauss and the steepest descent methods to get a fast convergence of the parameter estimates.

In the following discussion the linearity or the nonlinearity of the model shall refer to the manner in which unknown parameters enter the equation describing the model.

The problem is to estimate the parameters $\bar{p}$ of the nonlinear algebraic model represented by,

$$\bar{y} = f(\bar{x}, \bar{p}) \tag{1}$$

where,

$\bar{y}$ = measurable dependent variable

$\bar{x} = (x_1, x_2, \ldots, x_m)$ = measurable independent variables

$\bar{p} = (p_1, p_2, \ldots, p_p)$ = parameters to be estimated.

The criterion that is used to obtain the best estimates of the parameters from a measured set of data is the "least squares" criterion. In this, the sum of the squares of deviations of predicted values from the measured values is minimized. Thus we minimize the functions given by

$$S = \sum_{i=1}^{N} (y_1 - \bar{y}_i)^2 \qquad (2)$$

where,

y_i = measured value of the dependent variable (data)

$\bar{y}_i$ = estimated value (from the model)

i = 1, ..., N denote the number of data points.

Most algorithms for estimating parameters for nonlinear models are centered around two basic approaches. On the one hand, the function may be expanded in terms of the Taylor's series and corrections on several parameters calculated on the assumpt on of local linearity. On the other, modifications based on the steepest descent method have been used. The first method is known for its slow convergence, especially if the initial guess is poor. The second method converges very slowly in the neighborhood of the minimum. Marquardt's method is an optimum interpolation between these two methods.

The mathematical basis for the Gauss and steepest descent methods are given before presenting the Marquardt's method modification.

(a) Gauss Method [1]

This is an iterative approach based on the linearization of a function $f(\bar{x}_i, \bar{p}) = \bar{y}_i$ by a truncated Taylor series expansion about $\bar{p}^n$. The vector $\bar{p}^n$ represents the values of the parameters after the n^{th} iterations. Subscript i refers to a specific data point.

An expansion around $\bar{x}_i$, $\bar{p}_n$ gives

$$f(\bar{x}_i, \bar{p}_{n+1}) = f(\bar{x}_i, \bar{p}_n) + \sum_{j=1}^{P} \frac{\partial f_i}{\partial p_j} h_{j,n} \tag{2}$$

where

$$h_{j,n} = p_{j,n+1} - p_{j,n} \tag{4}$$

Hence, from equation (2)

$$S = \sum_{u=1}^{N} \left[y_i - f(\bar{x}_i, \bar{p}_n) - \sum_{j=1}^{P} \frac{\partial f_i}{\partial p_j} h_{j,n} \right]^2 \tag{5}$$

At the minimum, $\frac{\partial S}{\partial p_j} = 0$ (6)

Therefore setting the partial derivative of S with respect to p_j equal to zero, we obtain

$$\frac{\partial S}{\partial p_j} = -2 \sum_{i=1}^{N} y_i - f(\bar{x}_i, \bar{p}_n) - \sum_{k=1}^{P} \frac{\partial f_i}{\partial p_k} h_{k,n} \quad \frac{\partial f_i}{\partial p_j} = 0 \tag{7}$$

Equation (7) is linear in $h_{k,n}$.

By defining, $B_{i,j} = \frac{\partial f_k}{\partial p_j}$, $i = 1, 2, \ldots, N$; $\quad j = 1, 2, \ldots, P$

and

$$\bar{f}_n = \begin{bmatrix} f(\bar{x}_1, \bar{p}_n) \\ f(\bar{x}_2, \bar{p}_n) \\ \cdot \\ \cdot \\ \cdot \\ f(\bar{x}_N, \bar{p}_n) \end{bmatrix}, \qquad \bar{h}_n = \begin{bmatrix} p_{1,n+1} - p_{1,n} \\ \cdot \\ \cdot \\ \cdot \\ p_{P,n+1} - p_{P,n} \end{bmatrix}$$

the $\bar{h}_n$ can be determined from the matrix equation

$$(B^T B)\ \bar{h}_n = B^T(\bar{Y} - \bar{f}_n)$$

or

$$\bar{h}_n = (B^T B)^{-1}\ B^T\ (\bar{Y} - \bar{f}_n) \tag{8}$$

where

$$\bar{Y} = [y_1, y_2, \ldots, y_N]^T$$

Thus, assuming initial parameter values, we determine the improved estimates of p_j given by,

$$p_{j,n+1} = p_{j,n} + h_{j,n}$$

convergence is attained when $\bar{h}_n$ approaches zero.

This method converges rapidly in the vicinity of the minimum, where linearization can be justified. However, if the initial guess is poor, the method is known to converge very slowly, oscillate widely or even diverge.

(b) Steepest Descent Method [1]

The method of steepest descent simply moves from the current trial value, in the direction of the negative gradient of ϕ. The components and direction of successive iterations is given by the row vector

$$\bar{g} = - \left(\frac{\partial S}{\partial p_1}\right), \ldots, \left(\frac{\partial S}{\partial p_P}\right) \qquad \sum_{i=1}^{P} \left(\frac{\partial S}{\partial p_P}\right)^2 \quad 1/2 \tag{9}$$

Thus, a search is made in the direction of the negative gradient of S, namely $\bar{g}$, which is at right angles to the direction given by the Taylor's series expansion, $\bar{h}$. The step size is so chosen as to give the minimum

S in the direction of $\bar{g}$.

In effect, this method seeks to calculate corrections such that at each iteration the value of S will decrease most rapidly.

This method is successful for elongated and highly distorted S surfaces. Hence any initial guess rapidly converges till we reach the vicinity of the minimum. In the neighborhood of the minimum however, where the S contours are approximately circular, too large a correction is applied in the direction. Hence, the method oscillates about the minimum.

Qualitative Analysis of the Problem:

In Marquardt's modification, an algorithm is devised in such a manner as to take advantage of the fast convergence of the steepest descent method in the early stages, and that of the Gauss method in the vicinity of the minimum.

The following characteristics are desirable

(1) The correction vector applied should be within 90° of the negative gradient of S, otherwise S will increase successively.

(2) As the search gets closer to the minimum, the correction vector must coincide with $\bar{h}$.

(3) In addition to choosing the direction, the step size should be controlled so that there is rapid convergence and minimum oscillation.

In the algorithm developed by Marquardt the direction and the step size are controlled simultaneously. The algorithm is based on three theorems due to Morrison [4]. For a detailed discussion of the theorems and their proofs, the reader is referred to the paper by Marquardt [1].

Usage of the Program Deck [2]

The Marquardt's method makes use of a Maximum Neighborhood [1], which performs an optimum interpolation between the Taylor series method

and the gradient method based upon the maximum neighborhood in which the truncated Taylor series gives an adequate representation of the nonlinear model. An algorithm for this method was developed by D. W. Marquardt [1] and later on a computer program called the 'Least Square Estimation of Nonlinear Parameters" was written by him. This program is available in the IBM SHARE program library under the number SDA 3094.01 (NLIN).

NLIN is a main program to fit $\bar{y} = f(x_1, x_2, \ldots, x_m, P_1, P_2, \ldots, P_P)$ to fit a vector y of observed values of the dependent variables given N observations $(y_i, x_{i,2}, x_{i,2}, .., x_{i,m})$, i = 1, 2, 3, ..., N. For each observation $\bar{x}_i$ is a vector of m independent variables at the i^{th} data point and y_i is the observed value of the dependent variable at the same point.

The program can process any number of problems in one execution. Options are provided to use either estimated or analytic partial derivatives of f with respect to b_j; to control the amount and detail of printing; to plot observed and predicted values of the dependent variable; to introduce constraints at any coefficient value; to obtain nonlinear confidence limits and to use either FORTRAN compatible or PL/1 compatible external routines.

The input to the program consists of the following data groups in the order specified:

(1) problem parameters

(2) initial guesses of the P parameters

(3) Values of the dependent and the independent variables at the N data points.

Besides the above data cards, two subroutines called the PCODE and the FCODE have also to be supplied by the user. A brief description of the problem parameters and the subroutines is presented below [2].

Problem Parameters

N = Number of data points

K = Total number of coefficients

M = Number of independent variables

IP = Number of constant coefficients

ITOFF = Maximum number of iterations allowed to search for a solution. If this number of iterations is reached, all information obtained is printed, with a message indicating the reason for termination.

NOPCODE = Constant for determining the use of analytic or partial derivatives. If NOPCODE $\geq$ 1, estimated derivatives will be used (PCODE will not be called); if NOPCODE $\leq$ 0, analytic derivatives will be used (PCODE will be called)

NUMDIGT = Number of significant digits to be used in testing for convergence. Value must be in the range $0 < NUMDIGT < 8$.

DEL = Multiplier for estimated derivatives calculations. DEL must be in the range $0 < DEL < 1$.

GAMCR = Criterion angle used in gamma-epsilon test.

The two user supplied subroutines PCODE and FCODE are described below

FCODE: The calling sequence for this subroutine is

CALL FCODE (Y,X,B,PRNT,F,I,RES,M,N,K) where M,N,K are the problem parameters as defined above. Y is the vector of length N containing the observed values of the dependent variable. X is the two dimensional (NxM) array of values of the M independent variables at the N data points. B is the vector of length K containing the current parameter values. FCODE computes the functional value for the I^{th} data point and stores it in F, given X and B. The residual is then stored in RES. For the problem of Chapter 4, the FCODE can be written as follows

```
SUBROUTINE FCODE (Y,X,B,PRNT,F,I,RES,M,N,K)
DIMENSION Y(N), X(M,N), B(K), PRNT(2)
PRNT(1) = B(1)*EXP (B(2)*X(1,I))
PRNT(2) = B(3)* EXP (B(4)*X(2,I))
F = PRNT(1) + PRNT(2)
RES = Y(I) - F
RETURN
END
```

PCODE: The calling sequence for this subroutine is

CALL PCODE(P,X,B,PRNT,F,I,M,N,K) where M,N,K are problem parameters as defined earlier. X,B,PRNT and I are values just used in FCODE, and F is the function value just computed by FCODE for the I^{th} data point. P is the vector of length K to be used by PCODE to store the values of the K partial derivatives of f with respect to p_j. For the problem of Chapter 4, the PCODE can be written as follows

```
SUBROUTINE PCODE (P,X,B,PRNT,F,I,M,N,K)
DIMENSION P(K),X(M,N),B(K),PRNT(2)
P(1) = EXP(B(2)*X(1,I))
P(2) = B(1)*X(1,I)*EXP(B(2)*X(1,I))
P(3) = EXP(B(3)*X(2,I))
P(4) = B(3)*X(2,I)*EXP(B(3)*X(2,T))
RETURN
END
```

An output for the above problem has been attached at the end of the appendix. For a more detailed discussion of the usage of NLIN, the reader is referred to the IBM SHARE library program by D.W. Marquardt [2].

ILLEGIBLE DOCUMENT

THE FOLLOWING DOCUMENT(S) IS OF POOR LEGIBILITY IN THE ORIGINAL

THIS IS THE BEST COPY AVAILABLE

ILLEGIBLE

THE FOLLOWING DOCUMENT (S) IS ILLEGIBLE DUE TO THE PRINTING ON THE ORIGINAL BEING CUT OFF

ILLEGIBLE

```
N #  10      K #   4      P #   0      M #   1      IFP #   1      GAMMA CRIT #  0.450E 02      DEL #  0.100E-04
FF #  0.400E 01      T #  0.200E 01      E #  0.100E-05      TAU #  0.100E 00      XL #  0.000E 00      ZETA #  0.100E-30

%  0< PARAMETERS      0.10000000E-06     0.11000000E 02     0.10000000E 01    -0.10000000E 01
 0.CCE 00                                                                                    0.10E 02
&                                                                                                &

PTP CORRELATION MATRIX
      1      1.0000     0.9991     0.2777     0.5933
      2      0.9991     1.0000     0.2632     0.5695
      3      0.2777     0.2632     1.0000     0.7490
      4      0.5933     0.5695     0.7490     1.0000

            PHI                S E             LAMBDA          ANALYTIC PARTIALS USED
       0.19587660E-01     0.57136770E-01     0.100E-01

INCREMENTS     0.41363070E-06     0.12532140E 01    -0.81560550E-01     0.72194450E-01
            PHI             LAMBDA          GAMMA           LENGTH
       0.35619310E-03     0.100E-01     0.455E 02     0.189E 00

INCREMENTS     0.43262700E-06     0.14273110E 00    -0.83945750E-01     0.78474930E-01
            PHI             LAMBDA          GAMMA           LENGTH
       0.14232940E-04     0.100E-02     0.465E 02     0.196E 00

%  1< PARAMETERS      0.53262700E-06     0.11142730E 02     0.91605420E 00    -0.92152500E 00
 0.CCE 00                                                                                    0.10E 02
&                                                                                                &

PTP CORRELATION MATRIX
      1      1.0000     0.9991     0.2879     0.6005
      2      0.9991     1.0000     0.2734     0.5772
      3      0.2879     0.2734     1.0000     0.7563
      4      0.6005     0.5772     0.7563     1.0000

            PHI                S E             LAMBDA          ANALYTIC PARTIALS USED
       0.14232940E-04     0.15401800E-02     0.100E-02

INCREMENTS    -0.10485290E-06     0.47356240E-01    -0.12915750E-03     0.58557680E-02
            PHI             LAMBDA          GAMMA           LENGTH
```

```
        0.67205510E-07     0.100E-02     0.558E 02     0.550E-02

INCREMENTS     -0.23594940E-06     0.31666180E 00    -0.15782310E-03     0.60683630E-02
                PHI              LAMBDA          GAMMA          LENGTH
        0.16717650E-05     0.100E-03     0.683E 02     0.839E-02

%  2< PARAMETERS      0.29667750E-06     0.11459390E 02     0.91589640E 00    -0.91545660E 00
 0.0CE 00                                                                                  0.10E 02
&                                                                                            &



PTP CORRELATION MATRIX
      1       1.0000     0.9992     0.2849     0.5950
      2       0.9992     1.0000     0.2712     0.5728
      3       0.2849     0.2712     1.0000     0.7569
      4       0.5950     0.5728     0.7569     1.0000

              PHI                  S E              LAMBDA         ANALYTIC PARTIALS USED
        0.16717650E-05     0.52785170E-03     0.100E-03

INCREMENTS     -0.12634150E-07     0.19753330E 00    -0.69776520E-05     0.47963060E-04
                PHI              LAMBDA          GAMMA          LENGTH
        0.50067390E-07     0.100E-03     0.612E 02     0.171E-02

INCREMENTS     -0.20440620E-07     0.22644670E 00    -0.87567760E-05     0.62253450E-04
                PHI              LAMBDA          GAMMA          LENGTH
        0.47778480E-07     0.100E-04     0.659E 02     0.201E-02

%  3< PARAMETERS      0.27623690E-06     0.11685830E 02     0.91588760E 00    -0.91539430E 00
 0.0CE 00                                                                                  0.10E 02
&                                                                                            &



PTP CORRELATION MATRIX
      1       1.0000     0.9993     0.2823     0.5907
      2       0.9993     1.0000     0.2691     0.5692
      3       0.2823     0.2691     1.0000     0.7569
      4       0.5907     0.5692     0.7569     1.0000

              PHI                  S E              LAMBDA         ANALYTIC PARTIALS USED
        0.47778480E-07     0.89236080E-04     0.100E-04
```

```
INCREMENTS      0.36140790E-08   -0.20931070E-01   -0.16984570E-06    0.11975180E-05
              PHI              LAMBDA            GAMMA             LENGTH
        0.44227290E-07    0.100E-04         0.807E 02         0.244E-03

INCREMENTS      0.37201120E-08   -0.21365450E-01   -0.14049340E-06    0.96793970E-06
              PHI              LAMBDA            GAMMA             LENGTH
        0.44199160E-07    0.100E-05         0.809E 02         0.250E-03

% 4< PARAMETERS      0.27995690E-06    0.11664470E 02    0.91588740E 00   -0.91539330E 00

              PHI                S E              LENGTH            GAMMA             LAMBDA          ANALYTIC PARTIALS USED
        0.44199160E-07    0.85828460E-04    0.250E-03         0.809E 02         0.100E-05
```

N #, 10 K # 4 P # 0 M # 1
FF # 0.400E 01 T # 0.200E 01 E # 0.100E-05 TAU # 0.100E 00

% 4< PARAMETERS 0.27995690E-06 0.11664470E 02 0.91588740E 00 -0.91539330E 00
0.00E 00 0.10E 02
& &

% 4< PARAMETERS 0.27995690E-06 0.11664470E 02 0.91588740E 00 -0.91539330E 00

OBS	PRED	DIFF			
0.91585470E 00	0.91588770E 00	-0.32961360E-04	0.27995690E-06	0.91588740E 00	0.00000000E 00
0.83586940E 00	0.83577150E 00	0.97930430E-04	0.89881960E-06	0.83577060E 00	0.99999960E-01
0.76261940E 00	0.76266470E 00	-0.45359130E-04	0.28857180E-05	0.76266190E 00	0.19999990E 01
0.69588400E 00	0.69595760E 00	-0.73611730E-04	0.92647820E-05	0.69594840E 00	0.29999980E 00
0.63511680E 00	0.63510030E 00	0.16510480E-04	0.29745170E-04	0.63507060E 00	0.39999980E 00
0.57971500E 00	0.57961360E 00	0.10144710E-03	0.95498800E-04	0.57951810E 00	0.49999980E 00
0.52902370E 00	0.52913150E 00	-0.10782480E-03	0.30660480E-03	0.52882500E 00	0.59999970E 00
0.48361030E 00	0.48355060E 00	0.59664240E-04	0.98437620E-03	0.48256620E 00	0.69999970E 00
0.44349730E 00	0.44351430E 00	-0.16987320E-04	0.31604030E-02	0.44035390E 00	0.79999970E 00
0.41198360E 00	0.41198090E 00	0.27418130E-05	0.10146670E-01	0.40183420E 00	0.89999960E 00

PHI	S E	LAMBDA	ANALYTIC PARTIALS USED
0.44199160E-07	0.85828460E-04	0.100E-01	

PTP INVERSE

1	0.99925360E-06	-0.39180880E 01	0.27163740E-03	-0.21451160E-02
2	-0.39180880E 01	0.15380900E 08	-0.10361300E 04	0.82347140E 04
3	0.27163740E-03	-0.10361300E 04	0.58685410E 00	-0.18173160E 01
4	-0.21451160E-02	0.82347140E 04	-0.18173160E 01	0.97129090E 01

PARAMETER CORRELATION MATRIX

1	1.0000	-0.9994	0.3547	-0.6886
2	-0.9994	1.0000	-0.3449	0.6737
3	0.3547	-0.3449	1.0000	-0.7612
4	-0.6886	0.6737	-0.7612	1.0000

B	STD ERROR	ONE - PARAMETER LOWER	ONE - PARAMETER UPPER	SUPPORT PLANE LOWER	SUPPORT PLANE UPPER
1	0.85796380E-07	0.10836410E-06	0.45154970E-06	-0.63228580E-07	0.62314250E-06
2	0.33660620E 00	0.10991250E 02	0.12337680E 02	0.10318040E 02	0.13010890E 02
3	0.65750090E-04	0.91575590E 00	0.91601890E 00	0.91562440E 00	0.91615040E 00
4	0.26748880E-03	-0.91592830E 00	-0.91485830E 00	-0.91646320E 00	-0.91432330E 00

NONLINEAR CONFIDENCE LIMITS

PHI CRITICAL # 0.16206350E-06

PARA	LOWER B	LOWER PHI	UPPER B	UPPER PHI
1	0.27093870E-06	0.16313740E-06	0.28898020E-06	0.16203080E-06
2	0.11619770E 02	0.21833420E-06	0.11698160E 02	0.14926250E-06
3	0.91573440E 00	0.16184840E-06	0.91604070E 00	0.16202680E-06
4	-0.91580520E 00	0.16189970E-06	-0.91498010E 00	0.16206990E-06

```
10  4  0  1  1  0
 0  C  4 50  0  0
```

REFERENCES

1. Marquardt, D. W., "An Algorithm for Least Square Estimation of Nonlinear Parameters," J. Soc. Ind. Appl. Math., 2, 431 (1963).

2. Marquardt, D. W., "Least Squares Estimation of Nonlinear Parameters," IBM SHARE Program Library No. SDA 3094-01.

3. Kowalic, J. and M. R. Osborne, "Methods for Unconstrained Optimization Problems," American Elsevier, 1968.

4. Morrison, D. D., "Methods for Nonlinear Least Square Problems and Convergence Proofs, Tracking Programs and Orbit Determination," Proc. Jet Propulsion Laboratory Seminar, 1 (1960).

Appendix IV

CALCULATION OF PECLET NUMBER FOR THE ABSORPTION CHAMBER OF THE WATER-VAPOR ELECTROLYSIS CELL.

The hydraulic diameter of the rectangular absorption chamber is given by

$$D = \frac{4A_c}{L_p}$$

where

A_c = area of cross section, ft^2

L_p = perimeter , ft

The dimensions of the ARC module are

Length = 4.75 cm

Width = 14.5 cm

Depth = 0.159 cm

The hydraulic diameter for the ARC module is therefore given by

$$D = \frac{4A_c}{L_p} = \frac{4x14.5x0.159}{2x(14.5+0.159)} \times \frac{1}{2.54x12} \text{ ft}$$

$$= 0.0103 \text{ ft}$$

For air at 75^oF, the viscosity is 0.00016 ft^2/sec [1]

For the ARC module, the, velocity of air though the chamber is approximately 8.4 ft/sec [2]. The Reynolds number can therefore be calculated to be

$$Re = \frac{uD}{\nu} = \frac{8.4x0.0103}{0.00016} = 510$$

For water diffusing into air the Schmidt number is 0.60 [1].

Therefore

$$Re.Sc = 510 \times 0.60 = 306$$

According to the Taylor-Aris correlation [3,4] the Peclet number for fluids in laminar flow regions is given by

$$\frac{1}{P_e} = \frac{1}{Re.Sc} + \frac{Re.Sc}{192}$$

$$= \frac{1}{306} + \frac{306}{192} = 0.626$$

This Peclet number is however equal to $\frac{vD}{E_z}$

The Peclet number, which is used in Chapter 4 is therefore equal to

$$0.626 \times \frac{L}{D} = 0.626 \times \frac{4.75}{0.29} = 9.6$$

REFERENCES

1. Perry, J. H., "Chemical Engineers Handbook," 4 ed., p 3-26, McGraw Hill, New York, 1950.

2. Smith, E. L. and T. Wydeven, Private Communication.

3. Aris, R., Proc. Roy. Soc. (London), 235A, 67 (1956)

4. Taylor, G. J., Proc. Roy. Soc. (London), 223A, 446 (1954)

Appendix V

CALCULATION OF PERCENT REDUCTION IN HUMIDITY AS PREDICTED BY DISPERSION, PLUG FLOW, AND COMPLETE MIXING MODELS

Complete Mixing ($P_e = 0$)

In this case a new expression has to be obtained from the basic mass balance equation. Following the notation of Chapter 4, the mass balance for the completely mixed case may be written as

$$uA_c C_o - uA_c C_{out} - k A_m (C_{out} - C_i) = 0 \qquad (1)$$

where

C_{out} = concentration of water vapor in air at the outlet,

$$\frac{\text{lb of water}}{\text{ft}^3 \text{ of air}}$$

A_m = matrix area for mass transfer, ft^2

Equation (1) may be written as

$$uA_c(C_o - C_i) - uA_c(C_{out} - C_i) - kA_m (C_{out} - C_i) = 0$$

or

$$(C_o - C_i) - \frac{kA_m}{uA_c} + 1 \quad (C_{out} - C_i) = 0 \qquad (2)$$

Now

$$\frac{kA_m}{uA_c} = \frac{kyL}{uA_c} = B$$

Therefore,

$$\frac{C_{out} - C_i}{C_o - C_i} = \bar{H}_{out} = \frac{1}{1+B} \qquad (3)$$

The percent reduction in humidity = $(1 - \frac{1}{1+B}) \times 100$

For B = 1, the percent reduction in humidity = $(1 - \frac{1}{2}) \times 100$

$= 50$

For B = 5, the percent reduction in humidity = $(1 - \frac{1}{1+5}) \times 100$

$= 83.3$

Dispersion Model

Case 1: $P_e = 10$, B = 1

$$m_1 = \frac{P_e}{2} + \frac{P_e}{2}\sqrt{1 + \frac{4B}{P_e}} = 10.9$$

$$m_2 = \frac{P_e}{2} - \frac{P_e}{2}\sqrt{1 + \frac{4B}{P_e}} = -0.9$$

$$A_1 = \frac{m_2 e^{m_2}}{m_2 e^{m_2}(1 - \frac{m_1}{P_e}) - m_1 e^{m_1}(1 - \frac{m_2}{P_e})} = 5.7 \times 10^{-7}$$

$$A_2 = \frac{-m_1 e^{m_1}}{m_2 e^{m_2}(1 - \frac{m_1}{P_e}) - m_1 e^{m_1}(1 - \frac{m_2}{P_e})} = 0.917$$

Equation (4.6) can now be written as

$$\bar{H} = 5.7 \times 10^{-7}\ e^{10.9\eta} + 0.917\ e^{-0.9\eta} \qquad (3)$$

The outlet humidity can be obtained by putting $\eta = 1$ in equation (3), i.e.

$$\bar{H}_{out} = 5.7 \times 10^{-7}\ e^{10.9} + 0.917\ e^{-0.9} = 0.40$$

Therefore, the percent reduction in humidity $= (1 - \bar{H}_{out}) \times 100$

$$= (1 - 0.4) \times 100$$

$$= 60$$

Case 2: $P_e = 10$, $B = 5$

$$m_1 = \frac{P_e}{2} + \frac{P_e}{2}\sqrt{1 + \frac{4B}{P_e}} = 13.65$$

$$m_2 = \frac{P_e}{2} - \frac{P_e}{2}\sqrt{1 + \frac{4B}{P_e}} = -\ 3.65$$

$$A_1 = \frac{m_2 e^{m_2}}{m_2 e^{m_2}\left(1 - \frac{m_1}{P_e}\right) - m_1 e^{m_1}\left(1 - \frac{m_2}{P_e}\right)} = 5.7 \times 10^{-9}$$

$$A_2 = \frac{-m_1 e^{m_1}}{m_2 e^{m_2}\left(1 - \frac{m_1}{P_e}\right) - m_1 e^{m_1}\left(1 - \frac{m_2}{P_e}\right)} = 0.73$$

Therefore,

$$\bar{H} = 5.7 \times 10^{-9}\ e^{13.65\eta} + 0.73\ e^{-3.65\eta}$$

At the outlet,

$$\bar{H}_{out} = 5.7 \times 10^{-9}\ e^{13.65} + 0.73\ e^{-3.65} = 0.024$$

Therefore, the percent reduction in humidity = $(1 - 0.024) \times 100$

$= 97.6$

Plug Flow Model ($P_e \to \infty$)

As $P_e \to \infty$, equation (4.4) reduces to

$$\frac{d\bar{H}}{d\eta} + B\bar{H} = 0$$

The solution is

$$\bar{H} = A_1 e^{-B\eta}$$

Using the boundary condition $\bar{H} = 1$ at $\eta = 0$, we have

$$A_1 = 1$$

Therefore,

$$\bar{H} = e^{-B\eta}$$

The outlet humidity is given by

$$\bar{H}_{out} = e^{-B}$$

Percent reduction in humidity = $(1 - e^{-B}) \times 100$

For B = 1, the percent reduction in humidity = $(1 - e^{-1}) \times 100$

$= 63.2$

For B = 5, the percent reduction in humidity = $(1 - e^{-5}) \times 100$

$= 99.4$

ACKNOWLEDGMENT

I wish to thank my major professor Dr. L. T. Fan for his constant encouragement, guidance and support. Thanks are also due to Dr. L. E. Erickson and Dr. C. L. Hwang for the review of the manuscript and the constructive suggestions during the course of this work. The National Aeronautics and Space Administration under Contract NGR-17-001-034 and the Air Force Office of Scientific Research under Contract F44620-68-0020 (Themis Project) provided the financial support which is gratefully acknowledged.

ANALYSIS AND OPTIMIZATION OF THE WATER-VAPOR ELECTROLYSIS CELL

by

BHUWAN CHANDRA PANDE
B. Tech., I. I. T., Kanpur, 1968

AN ABSTRACT OF A MASTER'S THESIS

submitted in partial fulfillment of the

requirements for the degree

MASTER OF SCIENCE

Department of Chemical Engineering

KANSAS STATE UNIVERSITY

Manhattan, Kansas

1971

ABSTRACT

In this work a theoretical analysis of the water-vapor electrolysis cell has been done. This cell is being considered by NASA as a means of providing breathable oxygen for space missions of long durations. A cell module has been developed by the Ames Research Center of NASA and has been shown to have a reliable performance after two thousand hours of testing.

Weight is a prime consideration in developing equipment for use in spacecrafts. An expression has been developed for the weight of the ARC module as a function of temperature and current density. The operating temperature and the current density have been found which minimize the total system weight. It has been shown that the cell should be operated at the least possible temperature and the maximum possible current density.

A model for the absorption chamber of the water-vapor electrolysis cell has been developed which is very simple and readily adaptable for use in control system studies. It has been shown as to how, with the help of a nonlinear parameter estimation technique the parameters of this model can be estimated. Artificially generated data have been used in the absence of the availability of actual experimental data to illustrate the applicability of the approach.

For an insight in the design of matrix type cells, the ionic transport in solid electrolyte matrix has been analyzed. A model has been developed which can predict the concentration distribution of hydrogen ions in such cells. A parameter has been identified in this model which affects the concentration distribution of hydrogen ions in solid electrolyte matrix type cells.